# Molecular orbital study of the bond-valence sum rule using Lewis-electron pair theory

**Fumihito Mohri**

Electronics Laboratory, Kaneka Corporation, 5-1-1, Torikai-Nishi, Setsu, Osaka, 566-0072, Japan

Correspondence e-mail:
fmohri@mb.infoweb.ne.jp

The bond-valence sum rule has been examined by molecular-orbital methods related to spin-coupling matrix theory [Okada & Fueno (1976). *Bull. Chem. Soc. Jpn*, **49**, 1524–1530], to give a new formulation of the Lewis-electron pair concept. It is shown that the 'pair-coupling population' between atoms $M$ and $X$ exhibits the same behaviour as the bond valence between them. A quantum chemical definition for bond valence is proposed and successfully applied to $Al_2Cl_6$, $Te_4Cl_{16}$ and $Al_2Be_3(SiO_3)_6$ (beryl). Using an alternative bond-valence definition it is shown that for oxides the bond valence can possibly be taken as the double pair-coupling population.

## 1. Introduction

The bond-valence sum rule is becoming increasingly important in inorganic chemistry (Brown, 2002). The present work aims to clarify the origin of this rule, by applying to inorganic crystals 'molecular theories' representing the concepts and methods that have been used in the study of molecules (Julg, 1978). Since Pauling (1929) the bond-valence sum rule has often been interpreted using the ionic model. However, typical compounds to which the rule is applicable are oxides consisting of O atoms and the electropositive atoms such as Be, B, Al, Si, P and S. Since these atoms have electronegativity values lying between 1.5 (Be, Al) and 2.5 (S), corresponding to bonds with oxygen having between 37 and 78% covalent character,[1] the ionic model is unrealistic. Actually, there are some studies suggesting that the bond valence originates from the covalent bond interaction. The Brown–Altermatt formula (Brown & Altermatt, 1985), the most commonly used empirical relation, originates from the relation for carbon–carbon bonds (Pauling, 1960). The previous work of Mohri (2000), hereinafter referred to as Part I, shows that it is possible to apply the bond-valence sum rule to organic compounds with carbon–carbon bonds. Lendvay (1989) regarded the quantity from the Brown–Altermatt formula as a kind of 'bond order' and used it in his molecular-orbital study. Brown & Shannon (1973) pointed out that the bond valence is directly related to the covalent character of metal–oxygen

---

[1] According to Pauling (1960), the degree of covalent character is estimated by $100\exp[-0.25(\Delta x)^2]\%$, where $\Delta x$ is the electronegativity difference.

bonds. Gibbs (1982) found a linear correlation between bond valence and Mulliken overlap population (Mulliken, 1955), which is a measure of covalent bond strength. Accordingly, the present work looks for the theoretical basis of the covalent interpretation of the bond-valence-sum rule and pursues the quantum mechanical quantity (called $x$ in this section) that satisfies the following three requirements:

(i) for pure covalent bonds such as the carbon–carbon bond in an organic compound, $x$ is numerically identical to the classical bond order (throughout this paper, the terms 'classical bond order' and 'classical valence' represent those proposed in the 19th century[2]);

(ii) the sum of $x$ around the central atom in a polyhedron (this term includes molecules and polyatomic ions in this paper) is conserved even if the polyhedron is distorted from its regular shape, and even if the coordination number changes (this requirement is the implicit proposition for the bond-valence sum rule);

(iii) the bond distance dependence of $x$ agrees with the empirical relations (Brown & Altermatt, 1985; Mohri, 2000). Theoretical studies on the bond-valence sum rule other than those referred to above have been reported by Burdett & McLarnan (1984), Urusov (1995), Jansen *et al.* (1992), Burdett & Hawthorn (1993), Rutherford (1998) and Preiser *et al.* (1999). These are quite different from the present work in approach and give no quantity satisfying the three requirements mentioned above.

Since a covalent bond is considered to be formed by sharing Lewis-electron pairs, any theory of the Lewis-electron pair should clarify the theoretical background of the bond-valence sum rule. Okada & Fueno (1975, 1976) proposed the 'spin-coupling matrix theory', which enables us to analyse Lewis-electron pair populations in molecules, *not requiring electron-pair localization, and not using the resonance concept* (Pauling, 1960). The next section introduces the essential points of the spin-coupling matrix theory, because this theory is little known.[3] Only closed-shell systems are dealt with throughout this paper. Polyhedra concerned in this paper are those containing one type of ligand atom (they are called 'homo-ligand polyhedra' in Part I).

## 2. Spin-coupling matrix theory and valence

### 2.1. Theory

Wiberg (1968) found a molecular-orbital quantity whose numerical behaviour is the same as the classical bond order (examples will be shown later). This quantity was used as a 'bond index' (Armstrong *et al.*, 1973), but its theoretical background was left unclear. Okada & Fueno (1975, 1976) thought that this index should be derived from an extended theory of the Lewis-electron pair concept. The author

[2] Here, the 'classical valence of atom $A$' is taken as the maximum number of H atoms which can bond to atom $A$. 'Classical bond order' is the fractional classical valence shared with each bond.

[3] A plain description of this theory was given by Okada (1977), but this was written in Japanese and therefore not widely accessible. Moreover, after this paper, Okada and Fueno discontinued their studies in this area.

understands that the basic premise of Okada and Fueno comes from their opinion that the conventional Lewis-electron pair concept does not obey the *Probability Interpretation* of quantum mechanics. A Lewis-electron *pair* is a kind of quantum-mechanical particle pair whose space distribution should be formulated in terms of *two-particle probability*: this is the probability of finding one particle **1** with spin $s_1$ in a volume $dv_1$ around position $r_1$ and another particle **2** with spin $s_2$ in a volume $dv_2$ around position $r_2$, when all other particles may occupy arbitrary spin-orbitals (Löwdin, 1955a,b). Chemists know that the one-electron distribution should be formulated as a probability; for example, 'the number of electrons' belonging to an atomic orbital indicates the probability of finding electrons on the atomic orbital. Nevertheless, when referring to Lewis-electron pairs, almost no chemists have been conscious of the two-particle probability. Thus, Okada and Fueno argue that the conventional concept of the Lewis-electron pairs is inappropriate and that its appropriate definition should be as the two-particle probability in terms of the quantum-mechanical second-order density matrix (Löwdin, 1955a,b). Using this logic, they pursued a general formulation which can be defined for any approximation theory (*ab initio* Hartree–Fock molecular-orbital theory, Hückel molecular-orbital theory, density-functional theory, valence-bond theory *etc.*) for electronic state calculation of many-electron systems (such a formulation is called 'approximation-free formulation'). They succeeded in finding it by:

(i) applying the 'spin-coupling operator $(-4/3)S(\sigma_1) \cdot S(\sigma_2)$' to the second-order density matrix that expresses the distribution of all types of electron-pairs (including the up-spin up-spin pairs and the down-spin down-spin pairs) and then

(ii) integrating over spin coordinates $\sigma_1$ and $\sigma_2$.

Moreover, Okada & Fueno (1976) expressed the population analysis for Lewis-electron pairs within the framework of the LCAO-MO method.

When the total wavefunction of a closed-shell system with $N$ electrons is approximated by a single Slater determinant, the *pair-coupling population* on an atomic orbital $\chi_r$, $Q_{rr}^0$, and that between atomic orbitals $\chi_r$ and $\chi_s$, $Q_{rs}^0$, are expressed as follows:

$$Q_{rr}^0 = \frac{1}{4}(\mathbf{PS})_{rr}^2, \quad Q_{rs}^0 = \frac{1}{2}(\mathbf{PS})_{rs}(\mathbf{PS})_{sr}, \quad (1)$$

where $\mathbf{P}$ is the density matrix and $\mathbf{S}$ is the overlap integral matrix. The elements of $\mathbf{P}$ and $\mathbf{S}$ are defined as $P_{rs} = 2\sum_i^{\text{occ}} c_{ir}c_{is}$ and $S_{rs} = \int \chi_r\chi_s \, dv$, respectively, where occ denotes the occupied molecular orbitals $\varphi_i$ ($i = 1, 2,..., N/2$) and $c_{ir}$ is the coefficient for atomic orbital $\chi_r$ in the molecular orbital $\varphi_i$. $Q_{rr}^0$ is the probability of finding a Lewis-electron pair on atomic orbital $\chi_r$, so that it is called the 'ionic term' in the papers of Okada & Fueno (1975, 1976). $Q_{rs}^0$ is the probability of finding a Lewis-electron pair in the 'overlap region $\chi_r\chi_s$', so that this is called the 'covalent term'. According to Mulliken population analysis (Mulliken, 1955), the orbital population $q_r$ (electron population on atomic orbital $\chi_r$) is defined as

**Table 1**
Some examples of Mulliken overlap population ($n_{AB}$), Coulson bond order ($P_{AB}$) and Okada bond order ($D_{AB}$).

The suffix '$AB$' is a symbol for a bonded atom pair. '*Ab initio*' denotes *ab initio* HF/STO-3G.

(i) $C_2H_6$, $C_2H_4$, $C_2H_2$

|  | $n_{AB}$(*ab initio*) | | $P_{AB}$(CNDO) | | $D_{AB}$(*ab initio*) | | $D_{AB}$(CNDO) | |
|---|---|---|---|---|---|---|---|---|
|  | C—C | C—H | C—C | C—H | C—C | C—H | C—C | C—H |
| $C_2H_6$ | 0.728 | 0.766 | 2.250 | 1.351 | 1.009 | 0.984 | 1.061 | 0.978 |
| $C_2H_4$ | 1.198 | 0.783 | 3.228 | 1.380 | 2.014 | 0.977 | 2.064 | 0.964 |
| $C_2H_2$ | 1.794 | 0.809 | 3.985 | 1.401 | 2.997 | 0.984 | 2.997 | 0.984 |

(ii) Sums of $n_{AB}$, $P_{AB}$ and $D_{AB}$ around the C atoms in $C_2H_6$, $C_2H_4$ and $C_2H_2$.

|  | $\Sigma n_{AB}$(*ab initio*) | $\Sigma P_{AB}$(CNDO) | $\Sigma D_{AB}$(*ab initio*) | $\Sigma D_{AB}$(CNDO) |
|---|---|---|---|---|
| $C_2H_6$ | 3.026 | 6.303 | 3.961 | 3.995 |
| $C_2H_4$ | 2.764 | 5.988 | 3.968 | 3.992 |
| $C_2H_2$ | 2.603 | 5.386 | 3.981 | 3.981 |

(iii) HF and $HF_2^-$, here $A$ = H, $B$ = F.

|  | $n_{AB}$(*ab initio*) | $P_{AB}$(CNDO) | $D_{AB}$(*ab initio*) | $D_{AB}$(CNDO) |
|---|---|---|---|---|
| HF | 0.390 | 1.292 | 0.956 | 0.946 |
| $HF_2^-$ | 0.233 | 0.897 | 0.487 | 0.457 |

$$q_r = \sum_s P_{rs}S_{rs}. \tag{2}$$

There is the following relation among $q_r$, $Q^0_{rr}$ and $Q^0_{rs}$

$$q_r = 2Q^0_{rr} + \sum_{s(\neq r)} Q^0_{rs}. \tag{3}$$

The pair-coupling population on atom $A$ and that between atoms $A$ and $B$ are obtained from

$$Q^0_{AA} = \sum_{r \geq s}^A Q^0_{rs}, \quad Q^0_{AB} = \sum_r^A \sum_s^B Q^0_{rs}. \tag{4}$$

$Q^0_{AA}$ and $Q^0_{AB}$ are related to the atomic population $q_A$ by

$$q_A = 2Q^0_{AA} + \sum_{B(\neq A)} Q^0_{AB}. \tag{5}$$

The net charge of atom $A$, $c_A$, is defined as $c_A = Z^N_A - q_A$, where $Z^N_A$ is the nuclear charge of atom $A$. As $Q^0_{AB}$ is always positive, it is not helpful in assessing the nature of the inter-action (bonding or anti-bonding) between $A$ and $B$. This judgement is usually possible by checking the sign of the Mulliken overlap population $n_{AB} = 2\sum_i^{occ}\sum_r^A\sum_s^B c_{ir}c_{is}S_{rs}$.

When zero-differential overlap (ZDO) type molecular orbitals such as CNDO-MO [with respect to ZDO and CNDO (see Pople & Segal, 1966, and references cited therein)] are chosen, the overlap integrals in (1) and (2) are set to be $S_{rr} = 1$ and $S_{rs} = 0$ ($r \neq s$). Thus, the relations corresponding to (1) and (3) are expressed as (6) and (7), respectively

$$Q^0_{rr} = \tfrac{1}{4}P^2_{rr}, \quad Q^0_{rs} = \tfrac{1}{2}P^2_{rs} \tag{6}$$

$$q_r = P_{rr} = \tfrac{1}{2}P^2_{rr} + \tfrac{1}{2}\sum_{s(\neq r)}^A P^2_{rs} + \tfrac{1}{2}\sum_s^B P^2_{rs}. \tag{7}$$

The Wiberg bond index between atoms $A$ and $B$ is $\sum_r^A \sum_s^B P^2_{rs}$. The net charge on atom $A$, $c_A$, is defined as $c_A = Z^C_A - \sum_r^A q_r$, where $Z^C_A$ is the core charge of the valence shell in atom $A$. The determination of whether an orbital is 'bonding or anti-bonding' is possible by checking the sign of the Coulson (Coulson, 1961) bond order $P_{AB} = \sum_r^A \sum_s^B P_{rs}$.

## 2.2. Bond order and valence

To introduce the quantity corresponding to classical bond order, the $H_2$ molecule is taken as an example. Its bonding orbital is $\varphi = (\chi_1 + \chi_2)/(2 + 2S_{12})^{1/2}$ [the ZDO form is $(\chi_1 + \chi_2)/2^{1/2}$]. We can confirm that $Q^0_{11} = Q^0_{22} = 1/4$, $Q^0_{12} = 1/2$. Thus, only half of one electron-pair in the $H_2$ molecule contributes to the H—H bond. This is due to the well known fact that when no account is taken of the configuration interaction (CI), molecular-orbital theory overestimates the ionic contribution.[4] As this example shows, since a pure single bond gives the covalent term of 1/2, the double covalent term ($2Q^0_{AB}$) can be recognized as an extended definition for the classical bond order. Hereafter, $2Q^0_{AB}$ is referred to as the 'Okada bond order' for closed-shell systems and denoted as

$$D_{AB} \equiv 2Q^0_{AB} = \sum_r^A \sum_s^B (\mathbf{PS})_{rs}(\mathbf{PS})_{sr}. \tag{8}$$

The ZDO form is $D_{AB} = \sum_r^A \sum_s^B P^2_{rs}$ (the same as the Wiberg bond index). Note that the factor 2 in $2Q^0_{AB}$ is valid only when CI is not included in molecular-orbital calculations.

Table 1 shows some examples of Mulliken overlap populations ($n_{AB}$), Coulson bond orders ($P_{AB}$) and Okada bond orders ($D_{AB}$). From (i) and (ii) in Table 1, we can see that $D_{CC'}$ and $D_{CH}$ are very close to the classical bond orders of C—C and C—H, respectively. However, neither $n_{AB}$ nor $P_{AB}$ exhibits the same behaviour as the classical bond order. Moreover, they are not 'approximation-free quantities', *i.e.* $n_{AB}$ is valid only for LCAO-MOs constructed with non-orthogonalized basis functions, and $P_{AB}$ only for ZDO-type LCAO-MOs. Hence, neither $n_{AB}$ nor $P_{AB}$ can be candidates for the electronic expression of bond valence.

The present study defines the valence of atom $A$, $V_A$, as

$$V_A = \sum_{B(\neq A)} D_{AB}. \tag{9}$$

This follows the 'other theory' mentioned in §2.4. In this study a modification is introduced. Here, the $CO_2$ molecule is taken as an example. CNDO/2 calculations for $CO_2$ give $D_{CO} = 1.970$

---

[4] When using the Heitler–London wavefunction for $H_2$, we obtain $Q^0_{11} = Q^0_{22} = 0$, $Q^0_{12} = 1$.

($P_{CO}$ = 3.307) and $D_{OO'}$ = 0.300 ($P_{OO'}$ = −0.860), where the suffix OO′ denotes 'between two O atoms'. This $D_{OO'}$ value does not come from a covalent bond represented with 'bond-line(s)': such Okada bond orders usually appear between non-bonded atoms. The bond valence is in principle defined only for atoms connected with bond line(s). Thus, in order to directly relate the Okada bond order to the bond valence, in this study the former is divided into a bond-line part, $D_{AB}$(bond), and a non-bond-line part, $D_{AB}$(non-bond). Using these quantities, the valence of atom $A$, $V_A$, is defined as

$$V_A = \sum_{B(\neq A)} D_{AB}(\text{bond}) + \sum_{B(\neq A)} D_{AB}(\text{non-bond}). \qquad (10)$$

The first term on the right side in (10) is called the *bond-line part of the valence* and is represented as $V_A^b$.

$$V_A^b = \sum_{B(\neq A)} D_{AB}(\text{bond}). \qquad (11)$$

For $CO_2$, $V_C^b = 2 \times 1.970 = 3.940$. $V_C$ is equal to $V_C^b$ in this case, since there are no other atoms except the two O atoms. $V_O^b = 1.970$, $V_O = 1.970 + 0.300 = 2.270$. The ratio $V_A^b/V_A$ is regarded as a measure of 'Lewis-pair localization'. The maximum value of $V_A$, $V_A$(max), appears when every atomic orbital population is unity and it is expressed as

$$V_A(\text{max}) = N_{AO}, \qquad (12)$$

where $N_{AO}$ is the number of atomic orbitals of atom $A$ involved in chemical bonding.

In the ZDO approximation, (10) can be expressed in terms of atomic orbital populations of only one atom (say, $A$)

$$V_A \simeq \sum_r^A (2P_{rr} - P_{rr}^2). \qquad (13)$$

In this formula, the intra-atomic term in (7), $(1/2)\sum_{s(\neq r)}^A P_{rs}^2$, is neglected, because for the central atom in a polyhedron this term is usually much smaller than the $(1/2)\sum_r^A P_{rr}^2$ term. Hereafter, the wording 'covalent term' is not used, because $D_{AB}$ does not always arise from a covalent interaction, as mentioned above.

### 2.3. Relation to the valence and charge

This section illustrates the nature of the newly defined valence using (13). Fig. 1 shows $V_r = 2P_{rr} - P_{rr}^2$, where $V_r$ represents 'the orbital valence' of atomic orbital $\chi_r$. In the context of the conventional valence concept, we can obtain valence values only for the cases of $P_{rr}$ = 0, 1 and 2 (the valences are 0, 1 and 0, respectively; see Fig. 1). The function $V_r$ connects smoothly the three points at $P_{rr}$ = 0, 1 and 2. Hence, the newly defined valence is regarded as an extension of the classical valence.

In order to clarify the relationship between the valence and the atomic charge, we first take ethane, $C_2H_6$, as shown in Table 1. CNDO/2 results of the orbital populations on C and H in $C_2H_6$ are $(2s)^{1.015}(2p_x)^{0.980}(2p_y)^{0.980}(2p_z)^{1.030}$ and $(1s)^{0.999}$, respectively. The valence of C is $V_C = 2 \times 1.015 - 1.015^2 + 2 \times (2 \times 0.980 - 0.980^2) + 2 \times 1.030 - 1.030^2 = 3.998 \simeq 4$. The net

charge is $c_C = 4 - (1.015 + 2 \times 0.980 + 1.030) = -0.005 \simeq 0$. For the H atom, we obtain $V_H \simeq 1$, $c_H \simeq 0$. Almost the same results are obtained with other hydrocarbons. In these compounds, the 'zero-charge state' corresponds to the 'valence-satisfied state'.

Next we consider an example of an inorganic solid: Jellison *et al.* (1977) analysed the electronic state of $B_2O_3$ glass by means of NMR on $B^{10}$, $B^{11}$ and $O^{17}$ nuclei, making some assumptions. The main results are shown in Table 2. The results of O(R) and B are analysed in this section (we will discuss again the $B_2O_3$ result in §5.6). O(R) is bonded to two B atoms (see Fig. 13). For O(R), the valence is $V_O = (2 \times 1.541 - 1.541^2) \times 2 + (2 \times 2.000 - 2.000^2) + (2 \times 1.640 - 1.640^2) = 2.005$. This is virtually equal to the classical valence of oxygen, whereas the net charge $c_O$ is $6 - (2 \times 1.541 + 2.000 + 1.640) = 6 - 6.732 = -0.732$, which is significantly different from zero. Note that although this O atom is not in the zero-charge state, the valence is equal to its classical value. Similarly, the B atom has $V_B = 2.945$ (or 2.949) $\simeq 3$ (classical value) and $c_B = +1.027$ (non-zero charge). Thus, the newly defined valence permits the coexistence of the non-zero charge and the classical valence.

Additionally, note the results for $HF_2^-$ shown in Table 1 (iii). $D_{HF}$ for the H—F bond in $HF_2^-$ is about half that in the HF molecule. This means that the sum of $D_{HF}$ around the bridging H atom, $V_H$, is close to the valence of a 'univalent H atom'. This is very similar to the bond-valence sum rule.

### 2.4. Another theory related to spin-coupling matrix theory

Several researchers have developed a similar theory independent of Okada and Fueno: Armstrong *et al.* (1973), Giambiagi *et al.* (1975), Mayer (1983, 1986*a,b*), Gopinathan & Jug (1983*a,b*), Lendvay (1989) and Siddarth & Gopinathan (1990). Their theory is called 'Giambiagi–Gopinathan–Mayer theory' (abbreviated as GGM theory throughout this paper). In this theory the quantity corresponding to $D_{AB}$ is usually expressed as $B_{AB}$ (Mayer, 1986*a*), whose definition is identical to (9). The valence defined as $V_A = \sum_{B(\neq A)} B_{AB}$ has often
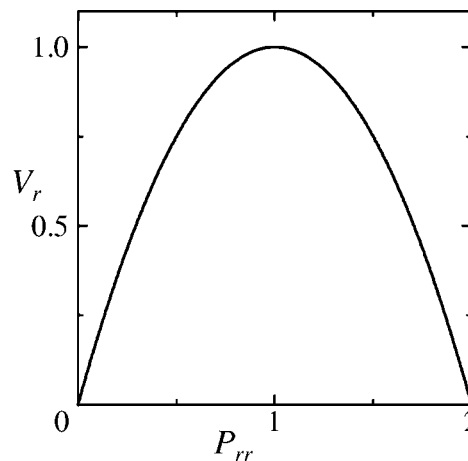


**Figure 1**
The relationship between orbital population ($P_{rr}$) and orbital valence ($V_r$); $V_r = 2P_{rr} - P_{rr}^2$ in ZDO form.

**Table 2**
Valence analysis for $B_2O_3$ glass using NMR data (Jellison *et al.*, 1977).

Here, $\sigma$ and $\sigma'$ denote $sp^2$ orbitals, $l$ lone-pair orbitals and $\pi$ $\pi$-orbitals. $V$ and $c$ are the total valence and the net charge, respectively.

| Atom | $\sigma$ (×2) | $l$ | $\sigma'$ | $\pi$ | $V$ | $c$ |
|------|------|------|------|------|------|------|
| O(R) | 1.541 | 2.000† | | 1.640 | 2.005 | −0.732 |
| B | 0.562 | | 0.489 | 0.360 | 2.945 | 1.027 |
| ‡ | 0.539 | | 0.535 | 0.360 | 2.949 | 1.027 |
| O(C) | 1.504 | 2.000† | | 2.000† | 1.492 | −1.008 |

† These populations are treated as an assumption by Jellison *et al.* (1977).   ‡ For the B atom two results are possible, owing to the 'sign-ambiguity' of the asymmetric factor for the electric field gradient.

been discussed in the papers on GGM theory (for example, Mayer, 1986*a*; Gopinathan & Jug, 1983*b*). Although both the spin-coupling matrix theory and GGM theory have their origin in the Wiberg bond index, they are different in their theoretical structure. In GGM theory

(i) there is no recognition that the Wiberg bond index should be related to the spin coupling and consequently the spin-coupling operator quoted above is not used;

(ii) there is no interpretation of $B_{AB}/2$ as the 'population of the Lewis-electron pairs', and

(iii) GGM theory is valid only in the framework of LCAO-MO theory.

However, as far as LCAO-MO methods are concerned, and as long as $2Q^0_{AB}$ is used as the bond order for closed-shell systems, both the spin-coupling matrix theory and GGM theory are the same, except that the ionic term $Q^0_{rr}$ is treated explicitly in the former. The present work uses the concepts, notations and terminology used in the spin-coupling matrix theory, but incorporates some results of studies using GGM theory.

## 3. Origin of valence conservation

### 3.1. The 'equal-population state'

Part I suggests that the conservation of the atomic population of the H atom in the hydrogen-bonded Cl—H···Cl systems is closely related to the bond-valence sum rule. Moreover, X-ray charge density analysis for kernite [$Na_2B_4O_6(OH)_2$·$3H_2O$; Cooper *et al.*, 1973] shows that both trigonal and tetrahedral B atoms have almost the same atomic charges (0.53 and 0.54, respectively). B—O systems are among those for which the bond-valence sum rule holds well (Donnay & Donnay, 1973). Hence, in this section we consider how to relate the atomic charge conservation to the valence conservation. The polyhedra concerned in this section and in §3.2 are those containing one type of ligand atom (hereafter called homo-ligand polyhedra). In §§3.1–3.3, we consider the cases where $D_{AB}$ (non-bond) terms are neglected and thus the relation $V^b_A = V_A$ holds.

From (13), the small variation of $V_A$, $\delta V_A$, for the small variation of orbital populations $\delta P_{rr}$ is derived as

$$\delta V_A = 2 \sum_r^A (1 - P_{rr}) \delta P_{rr}. \tag{14}$$

The atomic population conservation is expressed as

$$\delta q_A = \sum_r^A \delta P_{rr} = 0. \tag{15}$$

The valence conservation $\delta V_A = 0$ and the population conservation (15) do not in general coexist with each other, but in the special case where every orbital population $P_{rr}$ takes the same value (written as $P^0$), both conservation conditions can coexist

$$\delta V_A = 2(1 - P^0) \sum_r^A \delta P_{rr} = 2(1 - P^0) \delta q_A = 0. \tag{16}$$

Hereafter, this special case is called *the equal-population state*. Next, it will be shown that the equal-population state brings about the maximum covalent interaction and the minimum electron–electron repulsion, using the CNDO approximation (this approximation is useful for semi-quantitative energetic consideration, because in this approximation the whole electronic energy is decomposed into intraatomic parts and interatomic parts, and both are concretely expressed).

In the CNDO approximation the inter-atomic energy is expressed as

$$E_{AB} = \sum_r^A \sum_s^B (2P_{rs}\beta_{rs} - \tfrac{1}{2}P_{rs}^2\gamma_{AB}) + \text{electrostatic energy,} \tag{17}$$

where $\beta_{rs}$ is the resonance integral and $\gamma_{AB}$ is the repulsion integral parameter between $A$ and $B$. The second term in parenthesis is the 'inter-atomic exchange energy' and is connected to the pair-coupling population, $Q^0_{AB}$

$$E^{\text{exch}}_{AB} = -\tfrac{1}{2} \sum_r^A \sum_s^B P_{rs}^2 \gamma_{AB} = -Q^0_{AB}\gamma_{AB}. \tag{18}$$

If the polyhedron with atom $A$ as the central atom is regular in shape, the total amount of $E^{\text{exch}}_{AB}$ around $A$ is

$$\sum_B E^{\text{exch}}_{AB} = -\gamma_{AB} \sum_B Q^0_{AB} = -\tfrac{1}{2}V_A\gamma_{AB}. \tag{19}$$

This states that the valence of the central atom contributes to the stability of the polyhedron through the exchange interaction. Here we consider what condition achieves the maximum valence for an atom $A$ having $N_{AO}$ valence atomic orbitals and an atomic population of $q_A$ (*i.e.* the electron population of atom $A$), where $\sum_{r=1}^{N_{AO}} P_{rr} = q_A$ (here the summation symbol $\sum_{r=1}^{N_{AO}}$ is used when the number of atomic orbitals is specified). Using $P_{rr}$ and (12), the valence of $A$, $V_A$, is written as

$$V_A = \sum_{r=1}^{N_{AO}} (2P_{rr} - P_{rr}^2). \tag{20}$$

For a given atomic population $q_6$ we obtain the orbital populations that achieve the maximum valence for $A$ by using

Lagrange's undetermined multiplier method for the following $F$

$$F = \sum_{r=1}^{N_{AO}} (2P_{rr} - P_{rr}^2) - \mu \left( \sum_{r=1}^{N_{AO}} P_{rr} - q_A \right), \quad (21)$$

where $\mu$ is the undetermined multiplier. Conditions $\partial F / P_{rr} = 0$ ($r = 1, 2,..., N_{AO}$) lead to the following simultaneous equations: $2 - 2P_{rr} - \mu = 0$ ($r = 1, 2,..., N_{AO}$). These equations lead to the solutions (22) and (23)

$$P_{rr} = \frac{q_A}{N_{AO}} \ (r = 1, 2, ..., N_{AO}), \quad (22)$$

$$V_A^{max}(q_A) = \sum_{r=1}^{N_{AO}} \left( 2\frac{q_A}{N_{AO}} - \frac{q_A^2}{N_{AO}^2} \right) = 2q_A - \frac{q_A^2}{N_{AO}}, \quad (23)$$

where $V_A^{max}(q_A)$ is the maximum valence at atomic population $q_A$ [checking the second derivatives for (21) shows that (23) gives the maximum of $V_A(q_A)$].

Next, we relate the electron–electron repulsion to the spin-coupling matrix theory. In the *CNDO* approximation, the intra-atomic electron–electron repulsion for an atom $A$, $W_{rep}(A)$, is written explicitly as

$$W_{rep}(A) = \frac{1}{2} \sum_{r}^{A} \sum_{s}^{A} (P_{rr}P_{ss} - \frac{1}{2}P_{rs}^2)\gamma_{AA}, \quad (24)$$

where $\gamma_{AA}$ is the repulsion integral on atom $A$, and the double summation includes $r = s$.

Among the terms in this repulsion energy, the term corresponding to $Q_{AA}^0$ is $(1/4) \sum_r^A P_{rr}^2 \gamma_{AA}$ (hereafter, called 'intra-orbital-repulsion energy'). This repulsion energy is not the same as the inter-electron-pair repulsion energy[5] used in the electron-pair repulsion model (Gillespie & Nyholm, 1957). (Hereafter this principle is called the 'the electron-pair repulsion principle'.) However, the smaller repulsion should be energetically more advantageous for atom $A$ and is therefore worth taking into account as a factor determining the stability of a polyhedron. For atom $A$, the intra-orbital repulsion energy, $E_{rep}$, is

$$E_{rep} = \frac{1}{4} \sum_{r}^{A} P_{rr}^2 \gamma_{AA} = Q_{AA}^0 \gamma_{AA}. \quad (25)$$

Through the same procedure as for $V_A$ (here the number of atomic orbitals is specified as $N_{AO}$), we can arrive at the conclusion that $E_{rep}$ takes its minimum value, $E_{rep}^{min}(q_A)$, when the equal-population state, $P_{rr} = q_A/N_{AO}$ ($r = 1, 2,..., N_{AO}$), is achieved

$$E_{rep}^{min}(q_A) = \frac{1}{4N_{AO}} q_A^2 \gamma_{AA} = Q_{AA}^0(min)\gamma_{AA}, \quad (26)$$

where $Q_{AA}^0(min) = 1/(4N_{AO})q_A^2$ is the minimum of the ionic term $Q_{AA}^0 = (1/4) \sum_{r=1}^{N_{AO}} P_{rr}^2$. Equations (22), (23) and (26) indicate that the equal-population state brings the maximum valence (*i.e.* the lowest exchange energy) and the minimum intra-orbital repulsion together.

---

[5] The formulation of the total electron repulsion energy in terms of the Lewis-electron pair theory has not been carried out yet, as far as we are aware.

The discussion of (17) and (26) is not an exact proof that the equal-population state is energetically the most stable state for a central atom in a polyhedron, because the energy components influencing the valence and the geometrical structure of the system are not only $E^{exch}$ and $E_{rep}$, but also other types of energy (for example, inter-atomic electrostatic energy). However, the following inference leads to the conclusion that the equal-population state should be energetically the most stable state. The electron-repulsion principle requires that the arrangement of the electron-pairs around the central atom in a polyhedron should be as symmetric as possible. This requirement leads simultaneously to the equal-population state. Hence, since the electron-repulsion principle often succeeds in predicting molecular structures with energetically the most stable states, it can be concluded that the equal-population state is energetically the most stable state. This conclusion is valid for isolated polyhedra (*i.e.* molecules and complexes), but in this study it is considered that this conclusion can be applied in principle to polyhedra in crystals.

Strictly speaking, the equal-population state is not exactly realised even when the atom of interest is in a three-dimensionally symmetric environment, because the energy levels of atomic orbitals generally depend on the type of orbital ($s$, $p$, $d$,...). Therefore, the 'real equal-population state' takes the form $(s)^\alpha (p_x)^\beta(p_y)^\beta(p_z)^\beta$ (usually, $\alpha > \beta$), for example. When $\alpha = \beta$ holds for the population of $(s)^\alpha(p_x)^\beta(p_y)^\beta(p_z)^\beta$ (other atomic orbitals are not considered here) in a tetrahedral coordination, this atom has four $sp^3$ hybrid orbitals and simultaneously takes an equal-population state. In discussions of hybrid orbitals, the directionality of each hybrid orbital is usually emphasized. On the other hand, this work focuses on the 'equality of orbital population'.

### 3.2. Valence conservation in distorted polyhedra

In distorted polyhedra it is predicted that, in general, the equal-population state of the central atom is no longer maintained and the valence should decrease from its maximum (note that the distorted structures considered here are *equilibrium structures*). We consider the relationship between the changes in the orbital populations, the valence ($V_A$) and the intra-orbital repulsion ($E_{rep}$). Here, we do not explicitly treat the non-symmetric arrangement of the ligand atoms. Instead, we treat the change in the electron population of the atomic orbitals. Let us represent the change in the ratio of the electron population on atomic orbital $\chi_r$ on atom $A$, $k_r$ ($r = 1, 2,..., N_{AO}$), supposing that $|k_r| < 1$ and the atomic population before distortion is $q_0$. Each orbital population on $A$ in a distorted polyhedron can be written as $P_{rr} = (q_0/N_{AO})(1 + k_r)$. Substituting $P_{rr}$ leads to (27) and (28), respectively

$$V_A = V_A^{max}(q_0) + \frac{2}{N_{AO}} \left( q_0 - \frac{q_0^2}{N_{AO}} \right) \sum_{r=1}^{N_{AO}} k_r$$

$$- \left( \frac{q_0}{N_{AO}} \right)^2 \sum_{r=1}^{N_{AO}} k_r^2, \quad (27)$$

$$E_{\text{rep}} = E_{\text{rep}}^{\min}(q_0)\left(1 + \frac{2}{N_{\text{AO}}}\sum_{r=1}^{N_{\text{AO}}} k_r\right)$$
$$+ \tfrac{1}{4}\gamma_{AA}\left(\frac{q_0}{N_{\text{AO}}}\right)\sum_{r=1}^{2N_{\text{AO}}} k_r^2. \tag{28}$$

The terms for $\sum_{r=1}^{N_{\text{AO}}} k_r^2$ in (27) and (28) are related to the sum of squares of the orbital population deviations, $\delta_q^2$

$$\delta_q^2 = \sum_{r=1}^{N_{\text{AO}}}(P_{rr} - q_0/N_{\text{AO}})^2 = (q_0/N_{\text{AO}})^2\sum_{r=1}^{N_{\text{AO}}} k_r^2. \tag{29}$$

Equations (27), (28) and (29) indicate that when the atomic population ($q_0$) is constant ($\sum_{r=1}^{N_{\text{AO}}} k_r = 0$), the occurrence of non-equal orbital populations always heightens both the exchange energy and the intra-orbital repulsion energy. Thus, the central atom tends to maintain its equal-population state, even if distortion of the polyhedron takes place. In other words, atoms in molecules or crystals tend to make their electron population states as spherical as possible.

Next we consider the effect of the atomic population change ($q_0$-change, the case where $\sum_{r=1}^{N_{\text{AO}}} k_r$ varies). When atom $A$ is an electropositive atom, the inequality $q_0 - q_0^2/N_{\text{AO}} > 0$ (*i.e.* $q_0 < N_{\text{AO}}$, the case corresponding to $P_{rr} < 1$ in Fig. 1) usually holds. In this case, the increase in atomic population brings an increase in $V_A$ and consequently lowers the interatomic exchange energy $E^{\text{exch}}$. However, the increase in the atomic population heightens the intra-orbital repulsion energy $E_{\text{rep}}$. The decrease in atomic population lowers the repulsion energy, but raises $E^{\text{exch}}$. Such opposite behaviours of the two types of energy should act as a 'controller' of the $q_0$ change. Hence, even if the polyhedra are distorted to other equilibrium structures, the valences of electropositive atoms tend to be conserved, and their orbital population states tend not to lie far from their equal-population states. In electronegative atoms where the inequality $q_0 - q_0^2/N_{\text{AO}} < 0$ ($q_0 > N_{\text{AO}}$, $P_{rr} > 1$ in Fig. 1) holds, both $E_{\text{rep}}$ and $E^{\text{exch}}$ exhibit a parallel behaviour to $q_0$ change. Thus, both energies make the case of the $V_A$ increase ($q_0$ decrease) energetically advantageous. Since the electronic structures of polyhedra are determined not only with $E_{\text{rep}}$ and $E^{\text{exch}}$, the $V_A$ increase may not always be realised. However, at least a $V_A$ decrease, which is the case where atomic charges become more negative, should be unlikely. Thus, we have seen that the $q_0$-change effect depends on the type of atom. The actual valences of electropositive and electronegative atoms in crystals may be determined by 'compromise' between these atoms.

Additionally, in atoms where the equation $q_0 - q_0^2/N_{\text{AO}} = 0$ ($q_0 = N_{\text{AO}}$, $P_{rr} = 1$ in Fig. 1) holds, their valences are well conserved even with changes in the atomic charge. Examples of such atoms are C atoms ($N_{\text{AO}} = 4$, $q_0 \simeq 4$, $V_C \simeq 4$) and H atoms ($N_{\text{AO}} = 1$, $q_0 \simeq 1$, $V_H \simeq 1$) in hydrocarbons.

### 3.3. Valence conservation for coordination number change

Valence conservation for coordination number change is expressed by

$$V_{MX}^b(\nu_1) = V_{MX}^b(\nu_2). \tag{30}$$

Here, $\nu_1$ and $\nu_2$ are coordination numbers for $MX_{\nu 1}$ and $MX_{\nu 2}$ polyhedra, respectively.

When, these polyhedra are regular in shape, (30) is explicitly represented as

$$\nu_1 D_{MX}(\nu_1) = \nu_2 D_{MX}(\nu_2). \tag{31}$$

Here, $D_{MX}(\nu)$ is the Okada bond order for the $M-X$ bond in $MX_\nu$. At the present stage, the theoretical derivation of (30) is not given, but it will be numerically examined in §5. Hereafter, we assume that (30) and (31) hold well.

### 3.4. Quantum chemical definitions of bond valence

We consider the bond valence definition in terms of Okada bond order. In (31), when $\nu_1$ is equal to the absolute value of the oxidation number of $M$, $Z_M$ (such an example is the Si atom of an $SiO_4$ tetrahedron in a mineral), the relation $Z_M/\nu_2 = D_{MX}(\nu_2)/D_{MX}(Z_M)$ is obtained. Here, $Z_M/\nu_2$ is Pauling's electrostatic bond strength. From this relation, we can draw the inference that the bond valence can be defined as the ratio of the Okada bond order to that for the 'reference system'. This inference leads to the following expression for the bond-valence sum rule

$$s_{MX} = \frac{D_{MX}}{D_{MX}(\text{ref})}, \quad \sum_M s_{MX} = Z_X. \tag{32}$$

Here, $D_{MX}(\text{ref})$ is the Okada bond order of the reference system. The problem is how to define the reference systems: here the Brown–Shannon definition (Brown & Shannon, 1973) is chosen. In this definition the reference systems are taken as experimentally determined polyhedra and the 'reference bond valences' are defined as the Pauling electrostatic bond strengths. For example, the reference system for $Al^{3+}-O^{2-}$ is a regular $AlO_6$ octahedron with an $Al-O$ distance of 1.91 Å and its reference bond valence is set to be $3/6 = 0.5$. The author understands that this reference bond-valence determination is 'scaling $D_{\text{AlO}}$ to 3/6'. Hence, $D_{MX}(\text{ref})$ in (32) is taken as $D_{MX}(\nu_{\text{ref}})/s_{MX}^0$, where $\nu_{\text{ref}}$ is the coordination number for the reference system (polyhedron) and $s_{MX}^0$ is $Z_M/\nu_{\text{ref}}$. Using this reference bond valence, the bond-valence sum rule is expressed as

$$s_{MX} = s_{MX}^0 \frac{D_{MX}}{D_{MX}(\nu_{\text{ref}})}, \quad \sum_M s_{MX} = Z_X. \tag{33}$$

This definition of the bond valence, $s_{MX}$, is '*the relative definition of bond-valence*' in this paper. If the proportionality $V_A^b \propto Z_A$ (here, $A$ denotes every atom in a crystal) holds numerically, (33) will be justified.

Next, we consider an alternative expression for the bond-valence sum rule. See *et al.* (1998) emphasized that the bond-valence sum (they called it the 'bond-order sum') depends on the specific ligands. The idea of 'specific ligand dependence of the bond-valence sum' originates only from the covalent interpretation of the bond-valence sum rule, because in the ionic interpretation of the rule the bond-valence sum around $M$ should be equal to $Z_M$ for any ligand atom $X$. If we define

the bond valence as the quantity exhibiting the specific ligand dependence, a probable expression is

$$s_{MX} = D_{MX}, \quad \sum_X s_{MX} = V_M^b, \quad \sum_M s_{MX} = V_X^b. \quad (34)$$

That is, the bond valence is the Okada bond order itself and the bond-valence sum is identical to $V_A^b$ ($A = M, X$). Here, it is not necessary to distinguish between the 'electropositive atom' and the 'electronegative atom'. We call this definition '*the absolute definition of bond valence*'. In this definition the reference system is no longer necessary. It is unlikely that valences ($V_A^b$) take the same values of $Z_A$, in general, because the nature of the bond $A-B$ depends on atom $B$. However, if the relation $V_A^b \simeq Z_A$ holds numerically in minerals such as the oxides to which the bond-valence sum rule has been successfully applied, (34) can be regarded as a definition of the bond-valence sum rule. Clearly, this definition is chemically more significant than the relative definition, because chemical bond-related quantities (bond distance, normal vibration frequency *etc.*) are governed not by the 'relative bond order', but by the absolute bond order. In the following sections the relative definition of bond valence will be examined and finally the absolute definition will be explored.

## 4. Calculation methods for the pair-coupling population

A molecular-orbital program that is appropriate to the purpose of the present study should satisfy the following requirements:

(i) it must be easily applicable to every type of compound, not only organic compounds but also inorganic compounds including transition metal complexes and metal alloys;

(ii) it can calculate the Lewis-pair populations ($Q_{AA}^0$, $Q_{AB}^0$);

(iii) it can perform geometry optimization, in order to obtain the exact relationship between Okada bond order and bond distance *for the equilibrium structure*.

There is no program that satisfies (i), (ii) and (iii) simultaneously. Hence, the following three programs are used in this study: *DVSCAT* for (i), *LWSPR* for (ii) and *PC-GAMESS* for (iii).

*DVSCAT* (Adachi *et al.*, 1978; Kowada *et al.*, 1998) is an implementation of the DVX$_\alpha$ method (discrete variational $X_\alpha$ method; Adachi *et al.*, 1978). This program generates numerical basis functions (these are treated as minimal basis functions), so that skill in selecting basis functions is not needed. Electrically neutral atoms were taken as initial atomic states at the start of the SCF calculation. One thousand sample points per atom were used for numerical integration. *LWSPR* (Nakagawa, 2000) is an auxiliary program which operates on a file output from *DVSCAT* to yield $Q_{AA}^0$ and $Q_{AB}^0$. The present version of *LWSPR* is applicable only to closed-shell systems.

*PC-GAMESS* (Granovsky, 1999) is the personal computer version of the *GAMESS* (US) QC package (Schmidt *et al.*, 1993), which is an implementation of the *ab initio* Hartree–Fock molecular-orbital method (hereafter, abbreviated as *ab initio* HF). The geometry optimization condition chosen was

the default one with $1 \times 10^{-5}$ Hartree Bohr$^{-1}$ of the maximum energy gradient for the Cartesian coordinates of atoms. Minimal basis functions of STO-3G and STO-3G* (STO-3G plus Cartesian-*d*-type polarization functions) were used for H to F and for Al to Cl, respectively, because these 'crude' basis functions can accurately reproduce observed molecular structures (Davidson & Feller, 1986; Tossel, 1987) within short computational times. In some cases the more precise 3-21G (3-21G*) and 6-31G (6-31G*) basis functions were used.

In fact, *PC-GAMESS* gives $q_A$ and $B_{AB}$ (corresponding to $D_{AB}$) by default. Nevertheless, *DVSCAT* was used for the calculations of the Lewis-pair-related quantities ($q_A$, $Q_{AA}^0$, $Q_{AB}^0$). The reason for this choice is that the author thinks that *DVSCAT* is more appropriate than *ab initio* HF methods for the purpose of the Lewis-pair population analysis (see *Appendix A*). All the molecular-orbital calculations in this work were performed on personal computers with MS-Windows95/98/ME/2000.

## 5. Discussion

### 5.1. Examination of the valence conservation

This section examines numerically the valence conservation for central atoms. In order to make the molecular-orbital analyses as reliable as possible, the systems with 'charge per atom' of less than 0.25 (for BF$_4^-$, it is 1/5 = 0.2; 0.25 is a tentative border line) were chosen under the assumption that the hypothetical polyhedra used in this section can model the real polyhedra found in inorganic crystals. The selected systems are listed in Table 3 with an indication of which are observed in nature. $[Al_4(OH)_{16}]^{4-}$ (Fig. 2) consists of two types of Al(OH)$_6$ octahedra and the results for No. 14 in Table 3 are the average over the two Al(OH)$_6$ octahedra. The results of No. 12 (Fig. 3) are for the central Al in Fig. 3. The quantities $\sigma_R$ and $\sigma_\theta$ in Table 3 are measures of the degree of distortion for a polyhedron and are defined as

$$\sigma_R = \left[ \sum_i (R_i - R_{av})^2 / N_R \right]^{1/2} \quad \text{(in Å)} \quad (35)$$

and

$$\sigma_\theta = \left[ \sum_j (\theta_j - \theta_{av})^2 / N_\theta \right]^{1/2} \quad \text{(in degrees)}, \quad (36)$$

where $R_i$, $R_{av}$ and $N_R$ are the bond distance, the arithmetic average of bond distances and the number of bond distances in a polyhedron, respectively. Similarly, $\theta_i$, $\theta_{av}$ and $N_\theta$ are the corresponding parameters for bond angles. Figs. 4–6 show examples of the distorted polyhedra listed in Table 3. In Table 3 the average bond distances ($R_{av}$) for Nos. 9–22 are in agreement with those found in actual crystals to within 2% (see Table 1 in Part I). For example, the average Al—O distance in $[Al_4(OH)_{16}]^{4-}$ (No. 14) of 1.881 Å deviates from the observed values (1.91 and 1.92 Å) from X-ray analysis (Dent Glasser & Giovanoli, 1972*b*). This level of deviation is

**Table 3**
Examination of the valence conservation for polyhedra $MX_\nu$ with *ab initio* optimized geometries.

$R_{av}$ denotes averaged $M-X$ distances in Å.

| No. | $MX_\nu$ | System | $R_{av}$ | $\sigma_R$ | $\theta_{av}$ | $\sigma_\theta$ | $q_M$ | $Q_{MM}^0$ | $V_M^b$ | $V_M$ |
|---|---|---|---|---|---|---|---|---|---|---|
| (1) | $CC_2$ | $H_3CCCH$ | 1.325 | 0.135 | 180.00 | 0.00 | 3.963 | 0.983 | 3.985 | 3.992 |
| (2) | $CC_2$ | $HCCCCH$ | 1.292 | 0.117 | 180.00 | 0.00 | 3.983 | 0.992 | 3.996 | 3.999 |
| (3) | $CC_3$ | $C_{10}H_8$ | 1.424 | 0.011 | 120.00 | 1.48 | 3.965 | 0.987 | 3.787 | 3.982 |
| (4) | $CC_3$ | $(CH)_4CCH_2$ | 1.436 | 0.083 | 120.00 | 11.03 | 3.927 | 0.969 | 3.918 | 3.977 |
| (5) | $CC_4$ | $C(CH_3)_4$ | 1.550 | 0.000 | 109.47 | 0.00 | 3.814 | 0.916 | 3.948 | 3.963 |
| (6) | $CC_4$ | $HC[C(CH_3)_3]_3$ | 1.578 | 0.024 | 109.32 | 4.49 | 3.836 | 0.930 | 3.899 | 3.952 |
| (7) | $BeO_4$ | $[Be(OH)_4]^{2-}$ | 1.634 | 0.000 | 109.49 | 2.23 | 1.161 | 0.085 | 1.965 | 1.982 |
| (8) | $BeO_4$ | $Be[(H_2O)_2(OH)]_2$ | 1.611 | 0.134 | 108.44 | 12.49 | 1.168 | 0.087 | 1.951 | 1.982 |
| (9) | $BO_4$ | $[B(OH)_4]^-$ | 1.472 | 0.000 | 109.50 | 2.74 | 1.952 | 0.240 | 2.925 | 2.944 |
| (10) | $BO_3$ | $B(OH)_3$ coplanar | 1.365 | 0.000 | 120.00 | 0.00 | 2.021 | 0.256 | 2.996 | 3.018 |
| (11) | $AlO_6$ | $[Al(OH)_6]^{3-}$ | 1.920 | 0.000 | 90.00 | 0.93 | 1.966 | 0.154 | 3.272 | 3.316 |
| (12) | $AlO_4$ | $[Al_5O_4(OH)_{12}]^{5-}$ | 1.725 | 0.046 | 109.31 | 5.60 | 2.009 | 0.151 | 3.293 | 3.414 |
| (13) | $AlO_4$ | $[Al(OH)_4]^-$ | 1.725 | 0.000 | 109.52 | 4.12 | 2.076 | 0.167 | 3.400 | 3.479 |
| (14) | $AlO_6$ | $[Al_4(OH)_{16}]^{4-}$ | 1.881 | 0.074 | 89.62 | 7.72 | 1.958 | 0.149 | 3.219 | 3.325 |
| (15) | $AlO_6$ | *trans*-$[Al(OH)_4(H_2O)_2]^-$ | 1.884 | 0.095 | 89.38 | 10.79 | 1.990 | 0.155 | 3.280 | 3.360 |
| (16) | $AlO_6$ | *cis*-$[Al(OH)_4(H_2O)_2]^-$ | 1.880 | 0.078 | 90.00 | 11.18 | 1.956 | 0.153 | 3.230 | 3.318 |
| (17) | $AlO_4$ | $Al(OH)_3(H_2O)$ | 1.730 | 0.104 | 108.22 | 11.32 | 1.969 | 0.153 | 3.264 | 3.327 |
| (18) | $SiO_6$ | $[Si(OH)_6]^{2-}$ | 1.786 | 0.000 | 90.00 | 1.12 | 2.726 | 0.289 | 4.240 | 4.296 |
| (19) | $SiO_4$ | $[SiO(OH)_3]^-$ | 1.639 | 0.088 | 109.12 | 6.88 | 2.961 | 0.332 | 4.544 | 4.596 |
| (20) | $SiO_4$ | $Si(OH)_4$ | 1.615 | 0.000 | 109.54 | 4.44 | 2.833 | 0.303 | 4.375 | 4.455 |
| (21) | $SiO_6$ | *trans*-$Si(OH)_4(H_2O)_2$ | 1.779 | 0.125 | 89.92 | 1.79 | 2.779 | 0.294 | 4.319 | 4.381 |
| (22) | $SiO_6$ | *cis*-$Si(OH)_4(H_2O)_2$ | 1.787 | 0.142 | 89.42 | 9.10 | 2.797 | 0.300 | 4.329 | 4.393 |

The names of (1)–(6) are as follows: propyne, butadiyne (diacetylene), naphthalene, fulvene, neopentane, tri-*tert*-butylmethane. The actual systems in the table are as follows: $B(OH)_3$: orthoboric acid (Zachariasen, 1954); $[B(OH)_4]^-$: $Ba[B(OH)_4]_2 \cdot H_2O$ (Kutschabsky, 1969); $[Al_5O_4(OH)_{12}]^{5-}$: this is a model for the $[AlO(OH)_2]^-$ chain in $\gamma$-Ba[AlO(OH)$_2$]$_2$ (Dent Glasser & Giovanoli, 1972*a*); $[Al_4(OH)_{16}]^{4-}$: $\alpha$-$Ba_2[Al_4(OH)_{16}]$ (Dent Glasser & Giovanoli, 1972*b*); $[Si(OH)_6]^{2-}$: $[Ca_3Si(OH)_6 \cdot 12H_2O](SO_4)(CO_3)$ (Edge & Taylor, 1971). The terms *cis* and *trans* for the octahedral complex $X_4Y_2$ refer to ligand $Y$.

significant in terms of the standard uncertainties from the X-ray analysis, but not for the calculation of the valence, which gives bond distances that are at best reliable only to within 2%. For example, the calculated valences of the B atoms in
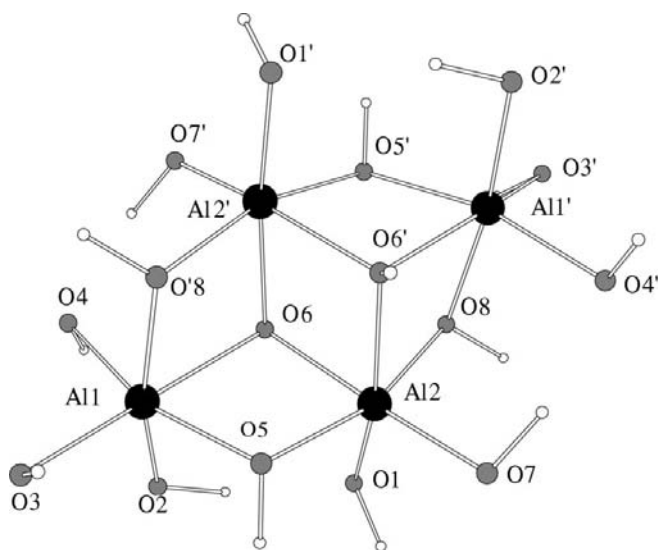
$BF_3$ are 2.893 (B−F = 1.313 Å, observed), 2.880 (B−F = 1.339 Å, 2% longer) and 2.861 (B−F = 1.287 Å, 2% shorter), showing the insensitivity of the valence to bond distance which is a result of using molecular orbitals without allowing for CI. In other words, in so far as near equilibrium structures are used for valence calculations by non-CI molecular-orbital methods, highly accurate agreements between calculated bond distances and observed ones are not always necessary (see also §5.3).

We can see from $\theta_{av}$ and $\sigma_\theta$ in Table 3 that the Al valences ($V_{Al}^b$ and $V_{Al}$) are virtually constant across systems 11–17, in spite of a large variation in the degree of angular distortion for $\sigma_\theta/\theta_{av}$ {the largest is 12.4% for *cis*-$Al[(OH)_4(H_2O)_2]^-$ (No. 16)}. The same tendency appears in the other systems. From Table 3 we can also see very little (or no) distance distortion ($\sigma_R$) dependence of $V_M^b$ and $V_M$ (Nos. 7 and 8 for $BeO_4$; Nos. 12, 13 and 17 for $AlO_4$; Nos. 11, 14 and 15 for $AlO_6$; Nos. 18, 21 and 22 for $SiO_6$). Thus, we can conclude that the valences defined by (9) and (11) for the central atoms of polyhedra are approximately conserved under polyhedron distortion.

From Table 3 we can also confirm that valence is conserved when the coordination number changes. For example, the valences ($V_M^b$ and $V_M$) of the six-coordinate Al and the four-coordinate Al fall within a narrow range of 3.23−3.40. The same feature appears in the B−O and Si−O systems. The atomic population ($q_M$) and the ionic term $Q_{MM}^0$ are also nearly conserved under polyhedral distortion and changes in coordination number.

### 5.2. Examination of the equal-population principle

Table 4 shows the *s*- and *p*-orbital populations of *M* (Be, B, Al, Si) in the selected systems in Table 3. Three organic
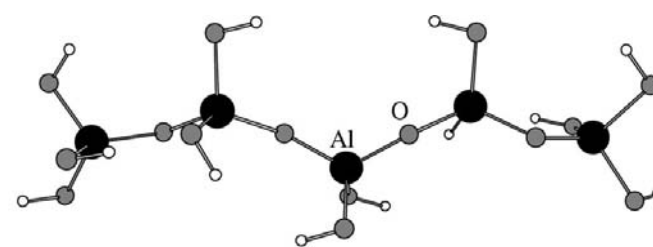


**Figure 2**
Calculated structure of $[Al_4(OH)_{16}]^{4-}$ (Dent Glasser & Giovanoli, 1972*a*, *b*). This structure has $C_i$ symmetry.



**Figure 3**
The calculated structure of $[Al_5O_4(OH)_{12}]^{5-}$ (No. 12 in Table 3). This is a model for $[AlO(OH)_2]^-$ chains in $\gamma$-Ba[AlO(OH)$_2$]$_2$ (Dent Glasser & Giovanoli, 1972*b*).

molecules are listed as typical examples of where near equal-population states are achieved. Table 5 shows the $3d$ orbital populations of Al and Si: the populations per orbital are much smaller than those of the $3s$ and $3p$ orbitals. This means that the $3d$-orbital contribution to Al—O and Si—O bonds is small, although its contribution to geometry optimization is known to be important (for example, see Tossel, 1987). Hence, it may be permissible to exclude the $3d$ orbitals of Al and Si from examination on the equal-population principle.

Considering Table 4 again, for the systems other than the organic compounds, in principle the $p$-orbital populations of the central atoms depend on the choice of the directions of the Cartesian coordinate axes since these polyhedra are distorted. However, given the condition that each ligand atom provides one lone pair of electrons to the central atom (*i.e.* there is no ligand atom that bonds especially strongly to the central atom), if the population state of $q_s \geq q_{px} \simeq q_{py} \simeq q_{pz}$ ($q_{px}$, for example, is the orbital population of $p_x$) appears in a coordinate system, such a population state should appear in any coordinate system. From Table 4 we can see that the near equal-population state is achieved and *cis*-$[\mathrm{Al(OH)_4(H_2O)_2}]^-$ (No. 16) is taken as an example. Although this $\mathrm{AlO_6}$ octahedron is markedly distorted ($\sigma_\theta/\theta_{av} = 12.4\%$), the orbital populations of the $3p$ orbitals of the Al are not far from each other and the population deviation ($100\delta^2 q$) is equal to that of $[\mathrm{Al(OH)_6}]^{3-}$ (No. 11), which has the smallest angular distortion ($\sigma_\theta = 0.93°$, $\sigma_\theta/\theta_{av} = 1.0\%$) among the Al—O systems. This same feature therefore appears in systems besides organic molecules.

An interesting feature is found in $\mathrm{B(OH)_3}$ and $\mathrm{B(OH)_4^-}$. If the conventional valence-bond view is applied to $\mathrm{B(OH)_3}$, the electron population of the B atom should be $(sp^2)^1 (sp^2)^1 (sp^2)^1 (2p_\pi)^0$ [this is identical to $(2s)^1 (2p_x)^1 (2p_y)^1 (2p_z)^0$]. However, the $2p_\pi$ orbital ($2p_z$ in this case) has an electron
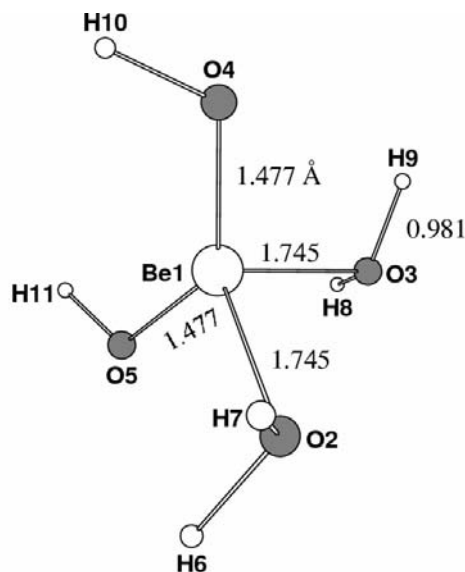
population of 0.473, matching those of the $2p_x$ and the $2p_y$ orbitals and consequently the near equal-population state is achieved. This situation is almost the same as in $[\mathrm{B(OH)_4}]^-$ (No. 9). Thus, the net charges and the valences of the trigonal B atom and the tetrahedral B atom in B—O systems are close to each other (see Table 3). This conclusion explains why the bond-valence sum rule is applicable to both trigonal and tetragonal B atoms.

### 5.3. Bond distance dependence of Okada bond order

As mentioned in §5.1, the calculated valence is insensitive to bond distance in a near equilibrium structure. This does not
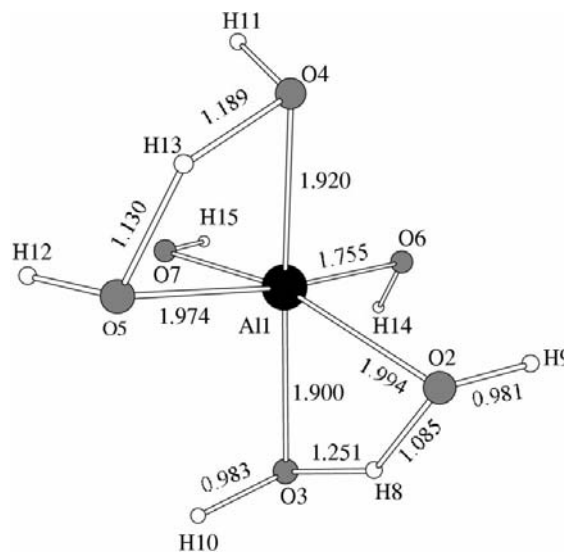


**Figure 5**
Calculated structure of *trans*-$[\mathrm{Al(OH)_4(H_2O)_2}]^-$ (No. 15 in Table 3). The bond distance Al1—O7 is 1.759 Å. The angle O2—Al1—O3 is 69.9° and O4—Al1—O5 69.3°. Other O—Al—O angles lie between 82.1 and 103.5°. Bond distances are given in Å.
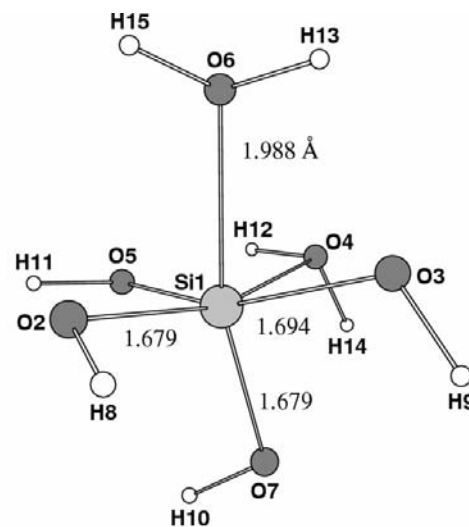


**Figure 4**
$\mathrm{Be(OH)_2(H_2O)_2}$ (No. 8 in Table 3). The bisector of O2—Be1—O3 is coincident with the $C_2$ axis. The O—Be—O angles lie between 95.88 and 134.32°. Bond distances are given in Å.



**Figure 6**
*cis*-$\mathrm{Si(OH)_4(H_2O)_2}$ (No. 22 in Table 3). The bisector of O4—Si1—O6 is coincident with the $C_2$ axis. Si1—O4 1.988, Si1—O5 1.694 Å. The O—Si—O angles lie between 76.7 and 107.0°. Bond distances are given in Å.

**Table 4**
Examination of the 'equal-population principle '.

The numbering is the same as that in Table 3. The descriptions for coordinate axes given here are incomplete, but are not necessary (see text).

| No. | $MX_v$ | $\sigma_\theta$ | $q_s$ | $q_{px}$ | $q_{py}$ | $q_{pz}$ | $100\delta^2 q$ | Coordinate |
|---|---|---|---|---|---|---|---|---|
| (1) | $CC_2$ | 0.00 | 1.071 | 0.938 | 0.984 | 0.970 | 0.97 | $x \parallel C-C$ axis |
| (3) | $CC_3$ | 1.48 | 1.101 | 0.936 | 0.950 | 0.979 | 1.70 | $x \parallel C-C$ axis |
| (5) | $CC_4$ | 0.00 | 1.098 | 1.012 | 1.023 | 1.026 | 0.46 | $y \parallel C-C$ axis |
| (8) | $BeO_4$ | 12.49 | 0.313 | 0.253 | 0.270 | 0.324 | 0.34 | $z \parallel Be-O$ axis |
| (7) | $BeO_4$ | 2.23 | 0.336 | 0.261 | 0.281 | 0.282 | 0.31 | $z \parallel Be-O$ axis |
| (10) | $BO_3$ | 0.00 | 0.544 | 0.502 | 0.502 | 0.473 | 0.26 | $z \perp BO3$ plane |
| (9) | $BO_4$ | 2.74 | 0.556 | 0.455 | 0.482 | 0.457 | 0.67 | $z \parallel B-O$ axis |
| (13) | $AlO_4$ | 4.12 | 0.548 | 0.322 | 0.296 | 0.301 | 4.42 | $x \parallel Al-O$ axis |
| (17) | $AlO_4$ | 11.32 | 0.522 | 0.304 | 0.297 | 0.274 | 4.03 | $z \parallel Al-O$ axis |
| (11) | $AlO_6$ | 0.93 | 0.533 | 0.293 | 0.293 | 0.287 | 4.40 | $x, y, z$ nearly $\parallel Al-O$ axes |
| (16) | $AlO_6$ | 11.18 | 0.533 | 0.281 | 0.316 | 0.283 | 4.40 | $z \parallel Al-O$, $y$ nearly $\parallel Al-O$ |
| (20) | $SiO_4$ | 4.44 | 0.711 | 0.444 | 0.425 | 0.428 | 5.85 | $z \parallel Si-O$ axis |
| (19) | $SiO_4$ | 6.88 | 0.740 | 0.431 | 0.447 | 0.454 | 6.24 | $z \parallel Si-O$ axis |
| (18) | $SiO_6$ | 1.12 | 0.716 | 0.413 | 0.410 | 0.418 | 6.65 | $x, y, z$ nearly $\parallel Si-O$ axes |
| (22) | $SiO_6$ | 9.10 | 0.719 | 0.433 | 0.425 | 0.409 | 6.63 | $z \parallel Si-O$ axis |

**Table 5**
$3d$-Orbital populations on the Al and the Si atoms of the systems in Table 3.

| No. | System | $q_{3dxy}$ | $q_{3dyz}$ | $q_{3dzx}$ | $q_{3dz^2 - r^2}$ | $q_{3dx^2 - y^2}$ |
|---|---|---|---|---|---|---|
| (11) | $[Al(OH)_6]^{3-}$ | 0.094 | 0.092 | 0.092 | 0.134 | 0.135 |
| (16) | $cis$-$[Al(OH)_4(H_2O)_2]^-$ | 0.064 | 0.136 | 0.092 | 0.141 | 0.117 |
| (13) | $[Al(OH)_4]^-$ | 0.152 | 0.097 | 0.151 | 0.116 | 0.092 |
| (17) | $Al(OH)_3(H_2O)$ | 0.099 | 0.090 | 0.120 | 0.153 | 0.103 |
| (18) | $[Si(OH)_6]^{2-}$ | 0.126 | 0.125 | 0.126 | 0.200 | 0.188 |
| (20) | $Si(OH)_4$ | 0.177 | 0.178 | 0.155 | 0.158 | 0.157 |

mean that the relationship between Okada bond order and bond distance does not correspond to the empirical relationship between the bond valence and bond distance, because empirical relationships such as the Brown–Altermatt relation (Brown & Altermatt, 1985) are valid only for observed structures in their equilibrium state. In other words, it is meaningless to examine the relationship between Okada bond order and Al—O distance in $[Al(OH)_6]^{3-}$, for example, by varying the Al—O distance. Hence, in order to compare the relationship between Okada bond order and bond distance with the empirical relation, we must use distorted equilibrium systems where the bond distance values are distributed over a wide range or equilibrium systems with different coordination numbers. Here, $[B_4O_5(OH)_4]^{2-}$ (Fig. 7) which occurs in borax (Morimoto, 1956), $[Al_4(OH)_{16}]^{4-}$ (No. 14 in Table 3) and hypothetical $Al(OH)_3$ are chosen.

Table 6 lists the bond distances for $M-O$ ($M$ = B, Al), Okada bond orders, $D_{MO}$, and the bond valence from the Brown–Altermatt formula, $s_{MO}$ (BA). Fig. 8 shows the relationship between the calculated bond distances and $D_{MO}$, $s_{MO}$ (BA). We can see that the $D_{MO}$ versus $R_{MO}$ relation is very close to the $s_{MO}$ (BA) versus $R_{MO}$ relation (dashed lines).

Next, we note the fact that there are some abnormal relationships between bond distance and bond order. Cyclobutane, $(CH_2)_4$, cyclopropane, $(CH_2)_3$, and spiropentane, $C(CH_2)_4$ (Fig. 9), are known as strained compounds and they have C—C—C angles that deviate strikingly from normal

values such as 109.5, 120 or 180°. Spiropentane, for example, has a very large angular distortion ($\sigma_\theta = 37.57°$, $\sigma_\theta/\theta_{av} = 31.8\%$). By comparison, neopentane, $C(CH_3)_4$, toluene, $C_6H_5CH_3$, biphenyl, $C_6H_5-C_6H_5$, and butadiene, $CH_2CHCHCH_2$, are taken as compounds having approximately normal C—C—C angles. Table 7 shows the C—C distances ($R_{CC}$) and the Okada bond orders ($D_{CC}$) in these hydrocarbons. All the C—C bonds concerned here are those which are drawn as single bond lines. From this table we can see that the $R_{CC}$ versus $D_{CC}$ relation in the 'abnormal' compounds is unusual, while the $R_{CC}$ versus $D_{CC}$ relation in the 'normal' compound is normal (i.e. as $R_{CC}$ increases, $D_{CC}$ decreases). Newton (1977) reported that the high-density region of the difference electron density distribution for a C—C bond in cyclopropane is shifted outward from the C—C—C triangle and a 'bent bond' is present. This means that the 'effective bond distance' is longer than the C—C internuclear distance. Thus, the presence of high strain may be a cause of the unusual $R_{CC}$ versus $D_{CC}$ relation.

Table 8 shows another type of abnormal relationship. For example, the C—C bond orders of (1)–(3) are shorter than the distance in ethane (6), in spite of the fact that the C—C distances of (1)–(3) are significantly shorter than that of ethane. If we consider only (1), (2) and (6), the following explanation may be possible. In $CF_3CH_3$ (1), for example, the covalency of the C—C bond has decreased, but the attractive
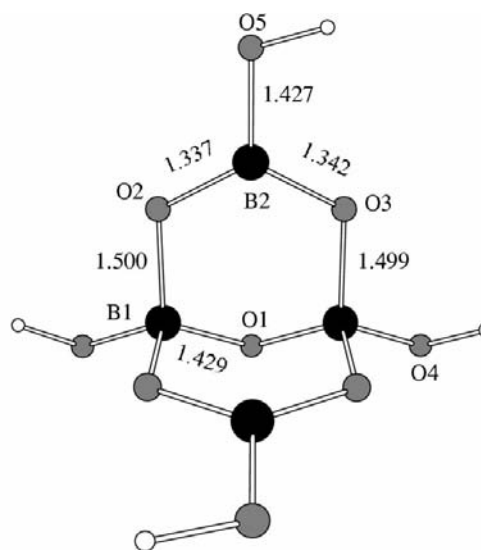


**Figure 7**
Calculated structure of $[B_4O_5(OH)_4]^{2-}$ in borax (Morimoto, 1956). The angles O2—B2—O are 116.4, 116.7 and 126.9°. The angles O—B1—O lie between 106.3 and 111.2°. Bond distances are given in Å.
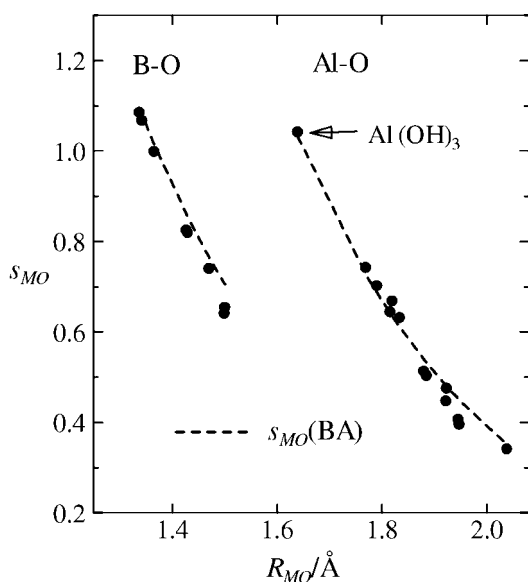
**Table 6**
Examination of the bond-distance dependence of the Okada bond order.

'HF' means *ab initio* HF/STO-3G optimization.

| $M-O$ | $R_{MO}$ (Å) X-ray | HF | $D_{MO}$ | $s_{MO}$(BA) | $n_{MO}$ |
|---|---|---|---|---|---|
| $[B_4O_5(OH)_4]^{2-}$ | | | | | |
| B1—O1 | 1.47 (3) | 1.429 | 0.819 | 0.855 | 0.622 |
| B1—O2 | 1.46 (3) | 1.499 | 0.651 | 0.708 | 0.486 |
| B1—O3 | 1.54 (3) | 1.500 | 0.644 | 0.715 | 0.496 |
| B1—O4 | 1.47 (3) | 1.470 | 0.740 | 0.776 | 0.559 |
| | 1.49 | 1.474 | 2.854 | 3.126 | |
| B2—O2 | 1.36 (3) | 1.337 | 1.085 | 1.111 | 0.766 |
| B2—O3 | 1.32 (3) | 1.342 | 1.067 | 1.096 | 0.752 |
| B2—O4 | 1.40 (3) | 1.427 | 0.825 | 0.871 | 0.607 |
| | 1.34 | 1.369 | 2.977 | 3.078 | |
| $[Al_4(OH)_{16}]^{4-}$ | | | | | |
| Al1—O2 | 1.88 (3) | 1.790 | 0.702 | 0.687 | 0.554 |
| Al1—O3 | 1.90 (3) | 1.819 | 0.668 | 0.635 | 0.522 |
| Al1—O4 | 1.88 (2) | 1.834 | 0.631 | 0.610 | 0.489 |
| Al1—O5 | 1.91 (2) | 1.922 | 0.447 | 0.481 | 0.367 |
| Al1—O6 | 1.98 (2) | 2.038 | 0.341 | 0.351 | 0.282 |
| Al1—O8' | 1.89 (2) | 1.923 | 0.475 | 0.479 | 0.352 |
| | 1.91 | 1.888 | 3.264 | 3.243 | |
| Al2—O1 | 1.85 (2) | 1.815 | 0.644 | 0.642 | 0.484 |
| Al2—O5 | 1.94 (5) | 1.885 | 0.503 | 0.531 | 0.416 |
| Al2—O6 | 1.93 (2) | 1.947 | 0.395 | 0.449 | 0.317 |
| Al2—O6' | 1.97 (2) | 1.945 | 0.406 | 0.452 | 0.347 |
| Al2—O7 | 1.87 (2) | 1.769 | 0.742 | 0.727 | 0.582 |
| Al2—O8 | 1.93 (2) | 1.880 | 0.513 | 0.539 | 0.429 |
| | 1.92 | 1.874 | 3.203 | 3.340 | |
| O6—H | | 0.977 | 0.875 | 0.773 | 0.603 |

$[B_4O_5(OH)_4]^{2-}$ is present in borax, $Na_2[B_4O_5(OH)_4]_2 \cdot 8H_2O$ (Morimoto, 1956).

electrostatic interaction is generated from the net charges with opposite sign. Hence, the 'short distance–small bond order' in (1) s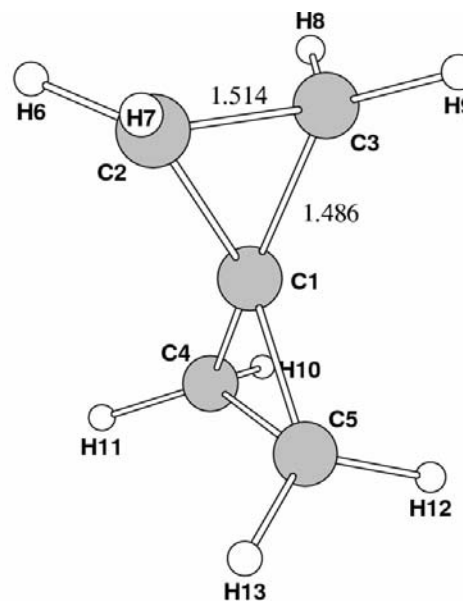eems to be ascribed to the difference in the electrostatic interaction. However, this explanation is not applicable to the combination of (3) and (6), nor does it explain the relationships between (4), (5) and (6). Presumably, in order to understand the abnormal relationship shown in Table 8, the influence of atoms other than the bonded atoms of interest should be taken into account. With respect to the application of the bond-valence sum rule to the determination of the 'effective oxidation numbers' in oxide superconductors, Jansen *et al.* (1992) proposed that 'cation–anion distances cannot be described in terms of valences (oxidation states, net charges) alone. Such distances depend sensitively on the changes in the environment...'. This opinion is essentially correct.

### 5.4. *d*-Orbital contribution to valence

Table 9 shows the effect of the $3d$ orbitals of $M$ ($M = Al^{3+}$ to $Cl^{7+}$ and $Fe^{2+}$, Fe$^0$, Co$^{3+}$ and Ni$^0$) on $V_M^b$ values as calculated using *DVSCAT*. Table 9 and Fig. 10 show the comparison between $V_M^b$ values ($M = Al^{3+}$ to $Cl^{7+}$) 'with $3d$ orbitals' and those 'without $3d$ orbitals'. $V_M^b$ 'with $3d$ orbitals' exhibit approximately linear correlation with the oxidation numbers and approximate continuity for the $V_M^b$ of Be, B and C, while $V_M^b$ 'without $3d$ orbitals' do not. This suggests that the $3d$ orbital contribution is necessary to the bond-valence sum rule for $Al^{3+}$ to $Cl^{7+}$ compounds. Thus, as shown in Table 4, although the $3d$ orbitals of $Al^{3+}$ to $Cl^{7+}$ compounds do not have a dominant role in $M-O$ bond formation, they significantly affect the valence values of the atoms in the compounds. Mayer (1987) reached the same conclusion for hypervalent sulfur using *ab intio* HF methods.

Among the transition metal complexes in Table 9, the valences of Fe and Co in (9)–(11) and (13) are much larger



**Figure 8**
The bond distance dependence of $D_{MO}$ ($M$ = B, Al) for $[B_2O_5(OH)_4]^{2-}$ (left curve) and $[Al_4(OH)_{16}]^{4-}$ (right curve). The added datapoint for Al(OH)$_3$ is indicated. The black circles denote $D_{MO}$.



**Figure 9**
HF/STO-3G structure of spiropentane. There are 'abnormal' C—C—C angles: C1—C3—C2 59.36, C2—C1—C3 61.28, C2—C1—C4 137.75°. The averaged C—C—C angle, $\theta_{av}$, around C1 is 112.26°. The angular distortion $\sigma_\theta/\theta_{av}$ around C1 is 37.57/112.26° × 100 = 31.8%.

**Table 7**
The relationship between the C—C distances and the Okada bond orders in the 'abnormal' and the 'normal' hydrocarbons.

$\theta$, $R$ and $D$ represent bond angle, bond distance and Okada bond order, respectively.

| 'Abnormal' | | | | 'Normal' | | |
|---|---|---|---|---|---|---|
| | $\theta_{CCC}$ (°) | $R_{CC}$ (Å) | $D_{CC}$ | | $\theta_{CCC}$ (°) | $R_{CC}$ (Å) | $D_{CC}$ |
| $(CH_2)_4$ | 89.9 | 1.553 | 0.988 | $C(CH_3)_4$ | 109.5 | 1.550 | 0.987 |
| $(CH_2)_3$ | 60.0 | 1.503 | 0.981 | $C_6H_5CH_3$ | 120.7 | 1.527 | 1.012 |
| $C(CH_2)_4$ | † | 1.513 | 0.980 | Biphenyl | 120.8 | 1.508 | 1.026 |
| | | 1.486 | 0.980 | Butadiene | 124.0 | 1.489 | 1.081 |

† See Fig. 9.

**Table 8**
Abnormal relationship between the bond order and C—C distances in halogenoethanes with observed structures (The Chemical Society of Japan, 1984).

$D$ and $c$ are Okada bond order and net charge, respectively.

| No. | | A | B | $R_{AB}$ (Å) | $D_{AB}$ | $c_A$ | $c_B$ |
|---|---|---|---|---|---|---|---|
| (1) | $CF_3CH_3$ | $C_F$ | $C_H$ | 1.494 | 0.990 | 0.970 | −0.422 |
| (2) | $CH_3CHF_2$ | $C_H$ | $C_{FH}$ | 1.498 | 1.000 | 0.650 | −0.368 |
| (3) | $CH_2FCH_2F$ | $C_{FH}$ | $C_{FH}$ | 1.503 | 0.985 | 0.203 | 0.203 |
| (4) | $CCl_3CH_3$ | $C_{Cl}$ | $C_H$ | 1.541 | 0.951 | 0.470 | −0.262 |
| (5) | $CF_3CCl_3$ | $C_F$ | $C_{Cl}$ | 1.54 | 0.857 | 0.887 | 0.282 |
| (6) | $CH_3CH_3$ | $C_H$ | $C_H$ | 1.535 | 1.035 | −0.148 | −0.148 |

**Table 9**
Examination of $3d$-orbital contribution to $V_M^b$ with values for Be, B and C given for comparison.

| No. | System | M | Without $3d$ | $V_M^b$ with $3d$-orbital population for 'with $3d$' |
|---|---|---|---|---|
| (1) | $Be(OH)_2(H_2O)_2$ | $Be^{2+}$ | 1.951 | |
| (2) | $B(OH)_3$ | $B^{3+}$ | 2.996 | |
| (3) | $CO_2$ | $C^{4+}$ | 3.849 | |
| (4) | $Al(OH)_3(H_2O)$ | $Al^{3+}$ | 2.332 | 3.264 |
| (5) | $Si(OH)_4$ | $Si^{4+}$ | 3.033 | 4.375 |
| (6) | $PO(OH)_3$ | $P^{5+}$ | 3.644 | 5.464 |
| (7) | $SO_2(OH)_2$ | $S^{6+}$ | 3.893 | 6.256 |
| (8) | $ClO_3(OH)$ | $Cl^{7+}$ | 3.770 | 6.579 |
| (9) | $[Fe(CN)_6]^{4-}$ | $Fe^{2+}$ | | 6.086 |
| (10) | $[Fe(Py)_6]^{2+}$ | $Fe^{2+}$ | | 3.812 |
| (11) | $[Fe(H_2O)_6]^{2+}$ | $Fe^{2+}$ | | 1.955 |
| (12) | $[Co(CN)_6]^{3-}$ | $Co^{3+}$ | | 5.654 |
| (13) | $[Co(NH_3)_6]^{3+}$ | $Co^{3+}$ | | 3.751 |
| (14) | $Fe(CO)_5$ ($D_{3h}$) | $Fe^0$ | | 6.195 |
| (15) | $Ni(CO)_4$ ($T_d$) | $Ni^0$ | | 4.620 |

Structural data are as follows: (3), (9), (12), (13), (14) and (15) are from *Kagaku-Binran* (The Chemical Society of Japan, 1984). (3): observed structure with C = O 1.16 Å. (6) HF/STO-3G* structure with P—$O_H$ 1.595, P=O 1.427 Å. (7) HF/3-21G* structure with S—$O_H$ 1.561, S=O 1.414 Å. (8) HF/3-21G* structure with Cl—$O_H$ 1.591, Cl=O 1.419 Å (av.). (9) observed structure with Fe—C 1.92, C—N 1.14 Å. (10) Pyridine (py) structure was determined with HF/STO-3G. The six pyridines were octahedrally arranged around Fe with Fe—N 2.036 Å (low spin). This distance is from See *et al.* (1998). (11) Fe—O 2.17 Å, estimated with the Brown–Altermatt (1985) relation. The $H_2O$ structure used here is the observed one. (12) observed structure with Co—C 1.894 Å. (13) observed structure with Co—N 1.970 Å. (14) observed structure with Fe—C 1.829 (×3), 1.809 (×2), C—O 1.153 Å. (15) observed structure ($T_d$) with Ni—C 1.84, C—O 1.13 Å.

than the oxidation numbers because of the large contribution of $3d$ orbitals. For example, the $3d$ orbital population state of Fe in $[Fe(CN)_6]^{4-}$ is $(3d_{xy})^{1.643}(3d_{yz})^{1.643}(3d_{zx})^{1.643}$-$(3d_{x^2-y^2})^{0.786}(3d_{z^2})^{0.786}$, where the population of each $3d_\pi$ orbital, 1.643, is significantly smaller than 2.000. This comes

from the presence of strong $3d_\pi$ (Fe)–$\pi*$ (CN) interactions. The conventional form of the bond-valence sum rule, which is formulated in terms of oxidation number, is not applicable to such atoms because the proportionality $V_A^b \propto Z_A$ is not achieved. As mentioned in §3.4, See *et al.* (1998) discussed the 'specific ligand effects' for the bond-valence sums of some first-row transition metal complexes. We can say that this effect is clearly shown in the $V_M^b$ of the $Fe^{2+}$ and $Co^{3+}$ complexes, if we regard the bond valence as the Okada bond order itself (see §5.6).

### 5.5. Bond-valence sums of electronegative atoms

**5.5.1. Reference systems**. The reference systems used hereafter are given in Table 10. To show that the selection of the reference systems is not uniquely determined, two candidate reference systems for Al—Cl are listed in Table 10. Since $V_{Al}^b$ are not exactly constant, the values of $s_{calc}$ for Al—Cl systems depend on the choice of reference system. The $TeCl_4$ molecule should be an appropriate reference system for $Te^{4+}$—$Cl^-$, but this monomeric molecule is unknown and *ab initio* HF calculations to determine the molecular structure of $TeCl_4$ gave unreasonable results. Hence, $[TeCl_6]^{2-}$ in $(NH_4)_2TeCl_6$ (Hazell, 1966) was chosen as the reference system for Te—Cl.

**5.5.2. Cl atoms in $Al_2Cl_6$ and $Te_4Cl_{16}$ molecules**. This section examines the bond-valence sums of Cl atoms in $Al_2Cl_6$ and $Te_4Cl_{16}$ (Buss & Krebs, 1971; Fig. 11), which are electroneutral molecules (they give reliable results from molecular-orbital calculations) but contain Cl atoms that form more
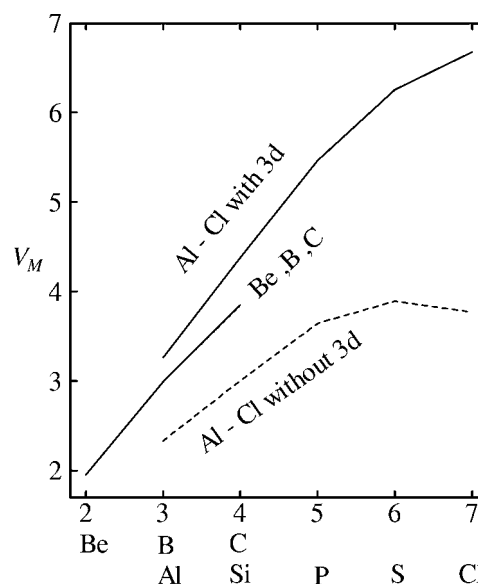


**Figure 10**
The contribution of $3d$ orbitals to the valences of $Al^{3+}$ to $Cl^{7+}$ for the compounds listed in Table 9, with values for Be, B and C for comparison.

**Table 10**
The reference systems $R_{MX}^0$ and $\lambda_{MX}$ are parameters used for the 'cubic relation' proposed in Part I.

| No. | $M-X$ | Reference system | Geometry | $R_{av}$ (Å) | $V_M^b$ | $D_{MX}$(ref) | $R_{MX}^0$ | $\lambda_{MX}$ (Å) | $s_0$ |
|---|---|---|---|---|---|---|---|---|---|
| (1) | H−O | $H_2O$ | Obs. | 0.96 | 0.870 | 0.870 | 0.96 | 0.09 | 1.000 |
| (2) | Be−O | $BeO_4$ systems† | HF/STO-3G | 1.61 | 1.958 | 0.490 | 1.63 | 0.40 | 0.250 |
| (3) | Al−O | $AlO_6$ systems† | HF/STO-3G* | 1.88 | 3.250 | 0.542 | 1.91 | 0.59 | 0.500 |
| (4) | Al−Cl | $AlCl_3$ | Obs. | 2.063 | 3.603 | 1.201 | 2.06 | 0.76 | 0.750 |
| (5) | | $AlCl_4^-$ | Obs. | 2.13 | 3.767 | 0.942 | 2.13 | 0.76 | 0.750 |
| (6) | Si−O | $SiO_4$ systems† | HF/STO-3G* | 1.615 | 4.361 | 1.090 | 1.63 | 0.50 | 1.000 |
| (7) | Te−Cl | $TeCl_6^{2-}$ | Obs. | 2.53 | 4.536 | 0.756 | 2.53 | 0.96 | 0.667 |

Geometry: Source of the observed structural data. $H_2O$: *Kagaku Binran*, 3rd ed. (The Chemical Society of Japan, 1984). $AlCl_3$: Aarset *et al.* (1999); $AlCl_4^-$: Table 1 in Part I. $[TeCl_6]^{2-}$: Hazell (1966). † The $M-O$ systems ($M$ = Be, Al, Si) are in Table 3.

**Table 11**
Examination of the bond-valence sum rule for Cl atoms in $Al_2Cl_6$ and $Te_4Cl_{16}$ which contain bridge-bonded Cl atoms.

| Molecules | $X-M$ | $R_{XM}$ (Å) | $D_{XM}$ | $s_{calc}$ | $s$(cubic) | $s$(BA) |
|---|---|---|---|---|---|---|
| $Al_2Cl_6$ | $Cl_t-Al$ | 2.04 | 1.184 | 0.986 | 0.92 | 0.979 |
| | $Cl_b-Al$ | 2.24 | 0.677 | 0.564 | 0.60 | 0.571 |
| $Te_4Cl_{16}$ | $Cl_t1-Te1$ | 2.315 | 1.146 | 1.011 | 1.03 | |
| | $Cl_t2-Te1$ | 2.311 | 1.149 | 1.013 | 1.05 | |
| | $Cl_t3-Te1$ | 2.317 | 1.159 | 1.022 | 1.03 | |
| | $Cl_b4-Te1$ | 2.908 | 0.382 | 0.337 | 0.35 | |
| | $Cl_b4-Te2'$ | 2.944 | 0.359 | 0.317 | 0.33 | |
| | $Cl_b4-Te2'$ | 2.959 | 0.343 | 0.302 | 0.32 | |

Source of structural data $Al_2Cl_6$: *Kagaku Binran*, 3rd ed. (The Chemical Society of Japan, 1984). $Te_4Cl_{16}$: Buss & Krebs (1971).

**Table 12**
Valence analysis for beryl, $Al_2Be_3(SiO_3)_6$, using the cluster model $[Be_4Al_4Si_6O_{15}(OH)_{22}]^{8-}$.

$c_A$ denotes the net charge of atom $A$. Averaged metal−oxygen bond distances (Å) were calculated with *ab initio* HF/STO-3G*. The corresponding observed values for Be−O, Al−O and Si−O are 1.653, 1.904 and 1.607 Å, respectively.

| Atom $A$ | Coordination | $R_{A-O}$ | $q_A$ | $c_A$ | $Q_{AA}^0$ | $V_A^b$ | $V_A$ |
|---|---|---|---|---|---|---|---|
| Be | $BeO_4$ tetrahedral | 1.601 | 1.116 | 0.884 | 0.079 | 1.831 | 1.919 |
| Al | $AlO_6$ octahedral | 1.883 | 1.890 | 1.110 | 0.137 | 3.108 | 3.232 |
| Si | $SiO_4$ tetrahedral | 1.617 | 2.773 | 1.227 | 0.287 | 4.242 | 4.397 |
| O1 | Bonding to 2Si | | 6.733 | −0.733 | 2.848 | 1.958 | 2.072 |
| O2 | Bonding to Be, Al, Si | | 6.751 | −0.751 | 2.863 | 1.934 | 2.050 |

bonds than their classical valence. Table 11 shows the results for $Al_2Cl_6$ and $Te_4Cl_{16}$. In this table, $s_{calc}$ is the bond valence calculated with (33), $s_{cubic}$ is given by the 'cubic formula', $s = s_0 (R^0 - \lambda)^3/(R - \lambda)^3$ (see Part I) and $s$(BA) comes from the formula of Brown & Altermatt (1985). In $Te_4Cl_{16}$, Te $5d$ orbitals are included in $DVX_\alpha$ calculations. Among 12 Te−Cl bonds in $Te_4Cl_{16}$, only the values for $Cl_t(1)$, $Cl_t(2)$, $Cl_t(3)$ and $Cl_b(4)$ ($t$ = terminal, $b$ = bridged) are listed in Table 11, because the results for the other Cl atoms are closely similar to these values. From Table 11, we can see that the $s_{calc}$ values are in good agreement with $s_{cubic}$ and $s$(BA)s. In $Te_4Cl_{16}$ especially, $s_{calc}$ ratios of the Te−$Cl_b$ and the Te−$Cl_t$ are very close to the expected value of 1/3.

**5.5.3. O atoms in beryl.** Beryl [$Al_2Be_3(SiO_3)_6$; Morosin, 1972] contains two types of O atoms, O1 and O2. O1 is shared

by two $SiO_4$ tetrahedra and O2 by one $BeO_4$ tetrahedron, one $SiO_4$ tetrahedron and one $AlO_6$ octahedron. O1 forms the same number of bonds as its classical valence, but O2 forms more. Pauling's electrostatic valence rule (the original form of the bond-valence sum rule) holds well for both these types of O atoms; 4/4 + 4/4 = 2, 2/4 + 4/4 + 3/6 = 2. In order to examine the bond-valence analysis for these O atoms, a cluster model $[Be_4Al_4Si_6O_{15}(OH)_{22}]^{8-}$ (Fig. 12) was made by the following procedure.

(i) The $[Be_4Al_4Si_6O_{37}]^{30-}$ cluster was extracted from the beryl structure. Since the structure of the cluster is as it is in beryl, it is not the equilibrium structure of an isolated cluster. In such a cluster, atomic valences should not take the values realised in its 'mother crystal'. Hence, the following steps were performed.

(ii) 22 protons were attached to terminal O atoms and O atoms shared by the $AlO_6$ octahedron and $BeO_4$ tetrahedron in order to reduce the negative charge.[6]

Through this process, the O atoms are categorized into four types:

(*a*) O shared by two $SiO_4$;
(*b*) O shared by one $BeO_4$, one $SiO_4$ and one $AlO_6$;
(*c*) OH bonding to $M$ ($M$ = Si, Be, Al);
(*d*) O shared by one $AlO_6$ and one $SiO_4$.

The O atoms of interest are (*a*) and (*b*).

(iii) Geometry optimization for the $[Be_4Al_4Si_6O_{15}(OH)_{22}]^{8-}$ cluster was carried out using HF/STO-3G*. Through this process, the structural parameters (bond lengths, bond angles) change from their original ones, but it is predicted from §5.1 that the valences of Be, Al, Si and the O atoms of (*a*) and (*b*) should approach those in beryl.

(iv) $DVX_\alpha$-MO calculations and Lewis-pair population analysis were performed for the proton-attached clusters with their optimized geometry.

Table 12 shows the result of the Lewis-pair population analysis. We can see that the valence ratio $V_{Be}^b:V_{Al}^b:V_{Si}^b:V_O^b$ is not far from the ratio of the classical valences (2:3:4:2). Next, considering O1 and O2 in Table 13, O1 bonds to two atoms, while O2 bonds to three (*i.e.* more than the classical valence of oxygen), but both O atoms have approximately the same valences. The sums of $s_{calc}$ of both O atoms (*ca* 1.8) are approximately 2, which is the ideal value for an O atom. However, there are significant discrepancies between $s_{calc}$ and $s$(BA), due to the 'abnormal relationship' discussed in §5.3. For example, the Okada bond order of 1.043 for O1−Si is smaller than that of 1.094 (4.375/4) for $Si(OH)_4$ in Table 3, despite the fact that the Si−O1 distance (1.593 Å) is shorter than the Si−O distance in $Si(OH)_4$ (1.615 Å).

**5.5.4. Oxygen atoms bonded to four atoms.** The O6 atom in $[Al_4(OH)_{16}]^{4-}$ (Fig. 2) bonds to three Al atoms and one H

---

[6] HF calculations for highly charged clusters often diverge.

**Table 13**
Bond-valence analysis for O atoms in beryl, $Al_2Be_3(SiO_3)_6$, using cluster model $[Be_4Al_4Si_6O_{15}(OH)_{22}]^{8-}$.

$s(BA)$: using $R_{OM}$(calc).

| O—M | $R_{OM}$(obs) (Å) | $R_{OM}$(calc) | $D_{OM}$ | $s_{calc}$ | $s(BA)$ |
|---|---|---|---|---|---|
| O2—Be | 1.653 | 1.586 | 0.452 | 0.461 | 0.575 |
| O2—Si | 1.620 | 1.616 | 1.094 | 1.018 | 1.022 |
| O2—Al | 1.904 | 1.990 | 0.385 | 0.355 | 0.411 |
| | | Sum | 1.931 | 1.835 | 2.008 |
| O1—Si | 1.592 | 1.593 | 1.043 | 0.957 | 1.088 |
| O1—Si′ | 1.594 | 1.628 | 0.915 | 0.839 | 0.990 |
| | | Sum | 1.958 | 1.798 | 2.078 |

atom. Since this environment is the same as that found in the crystal for $Ba_2[Al_4(OH)_{16}]$, it is considered that this O atom has essentially the same valence as in the crystal. Each Okada bond order can be found from Table 6. O6 accepts Okada bond orders of 0.880 from the H atom, and 0.341 + 0.395 + 0.406 = 1.142 from the three Al atoms. The bond-line valence is $V_O^b = 2.022$ and the bond-valence sum is 0.5 × (1.142/0.543) + 1.0 × 0.880/0.870 = 2.062 (*i.e.* close to 2). Thus, including the results from §§5.5.2 and 5.5.3, we can conclude that for electronegative atoms the Okada bond order exhibits nearly the same behaviour as the bond valence.

## 5.6. Examination of the absolute definition for bond valence

**5.6.1. Comparison of experimental and theoretical valences**. In order to examine the absolute definition of the bond valence, we need experimental valences against which to 'calibrate' the theoretical valences. However, and unfortunately, as far as the author is aware the only experimental results available for this purpose are those of Jellison *et al.* (1977) quoted in §2.3. Therefore, the considerations outlined in this section rely solely on this one experimental study. Generally speaking, experimental results act as checks on theoretical results. However, since the experimental results of Jellison *et al.* are based on some unavoidale assumptions, the
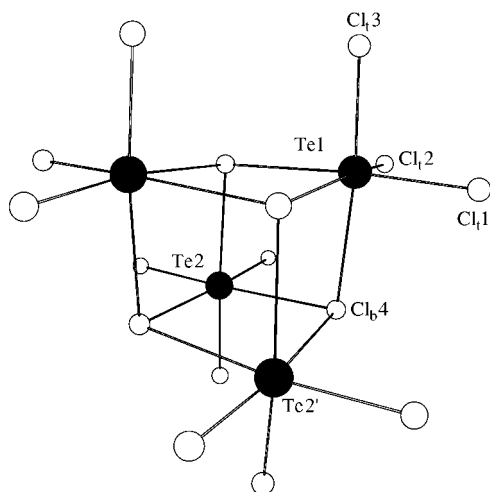


**Figure 11**
Molecular structure of $Te_4Cl_{16}$ (Buss & Krebs, 1971).

**Table 14**
Atomic orbital coefficients in localized molecular orbitals for the $\pi$ and lone pair orbitals of O(C).

Here, O7 is O(C).

| AO No. | AO | O7 $l$ | O7 $\pi$ |
|---|---|---|---|
| 16 | O 4 S | 0.0072 | −0.0054 |
| 17 | O 4 S | −0.0506 | 0.0367 |
| 18 | O 4 X | 0.0050 | −0.0074 |
| 19 | O 4 Y | −0.0235 | 0.0429 |
| 20 | O 4 Z | −0.0323 | −0.0381 |
| 21 | B 5 S | 0.0016 | 0.0113 |
| 22 | B 5 S | 0.0308 | −0.0247 |
| 23 | B 5 X | −0.0555 | 0.0437 |
| 24 | B 5 Y | −0.0850 | −0.0480 |
| 25 | B 5 Z | 0.0366 | **0.2012** |
| 31 | O 7 S | **0.1907** | 0.0005 |
| 32 | O 7 S | **−0.7637** | −0.0019 |
| 33 | O 7 X | **−0.0041** | 0.0619 |
| 34 | O 7 Y | **−0.6514** | 0.0009 |
| 35 | O 7 Z | 0.0000 | **0.8795** |
| 46 | B 10 S | 0.0016 | −0.0113 |
| 47 | B 10 S | 0.0306 | 0.0249 |
| 48 | B 10 X | 0.0542 | 0.0445 |
| 49 | B 10 Y | −0.0862 | 0.0483 |
| 50 | B 10 Z | −0.0370 | **0.2007** |
| 53 | O 13 S | −0.0065 | −0.0035 |
| 54 | O 13 S | 0.0435 | 0.0257 |
| 55 | O 13 X | 0.0328 | 0.0165 |
| 56 | O 13 Y | −0.0059 | −0.0321 |
| 57 | O 13 Z | 0.0232 | −0.0422 |

25 atomic orbitals (AOs) were selected from 89 AOs. '$S$, $S$, $X$, $Y$ and $Z$' represent $1s$, $2s$, $2p_x$, $2p_y$ and $2p_z$. The coefficients in bold are those for the main atomic orbitals.

conclusions cannot be regarded as strict checks and it is therefore reasonable to check the experimental result by a theoretical method (*i.e.* a molecular-orbital method). It is known that the structure of vitreous $B_2O_3$ consists of planar boroxol rings ($B_3O_6$) and $BO_3$ triangles (for example, Suzuya *et al.*, 2000). Thus, four types of oxygen are possible:

(i) oxygen contained within a boroxol ring;
(ii) oxygen bridging boroxol rings;
(iii) oxygen bridging two $BO_3$ triangles;
(iv) oxygen bridging a boroxol ring and a $BO_3$ triangle.

According to an $O^{17}$ NMR study by Youngman *et al.* (1995), the population fractions of these types of oxygen are 0.5, 0.3, 0.2 and 0 for (i), (ii), (iii) and (iv), respectively, so that the 'two-boroxol ring model' includes 80% of the O atoms in $B_2O_3$ glass. Hence, it may be permissible to choose this 'two-boroxol ring model' to simulate the results of Jellison *et al.* (1977). Fig. 13 shows the model whose structure was determined using *ab initio* HF/STO-3G. The B5—O7—B10 'bridging angle' of 130.50° is in good agreement with the value (130°) quoted by Jellison *et al.* (1977).[7]

The valence calculations were carried out for several values of the twist angle ($\varphi$). The calculated valences and the net charges exhibited very little $\varphi$ dependence, so the results at the equilibrium twist angle ($\varphi = 27.78°$) are discussed in this section. The total valences from $DVX_\alpha$ are 2.005, 2.928 and

---

[7] The experimentally determined bridging angles are actually distributed over a wide range in $B_2O_3$ (Suzuya *et al.*, 2000) and thus Jellison *et al.*'s results for O(C) are affected by this wide distribution.

2.050 for O(R), B, O(C), respectively. Comparing these values with those in Table 2, we can see that for O(R) and B the calculated valences are in good agreement with their 'experimental values', but the value for O(C) is not. The source of this discrepancy for O(C) lies mainly in the assumption of a doubly occupied $\pi$-orbital for O(C). Actually, the orbital population of the $\pi$-orbital of O(C) ($2p_z$ of O7) is 1.745, significantly smaller than 2. In order to find the reasons for this value, the localized molecular orbitals (LMO; Edmiston & Ruedenberg, 1963) for the molecular orbitals from *ab initio* HF/STO-3G were calculated using *PC-GAMESS* (strictly speaking, the localized orbitals for DVX$_\alpha$ molecular orbitals should be obtained here, but the present version of *DVSCAT* has no such facility). Table 14 lists the LMOs corresponding to the $\pi$-orbitals and the lone-pair
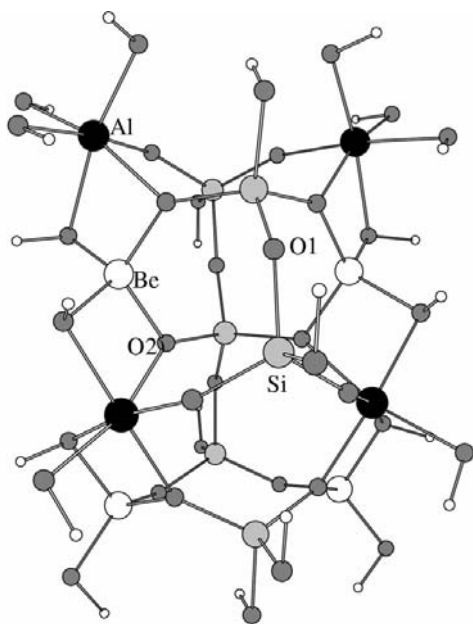


**Figure 12**
Calculated structure of $[Be_4Al_4Si_6O_{15}(OH)_{22}]^{8-}$, a cluster model for beryl, $Al_2Be_3(SiO_3)_6$ (Morosin, 1972).



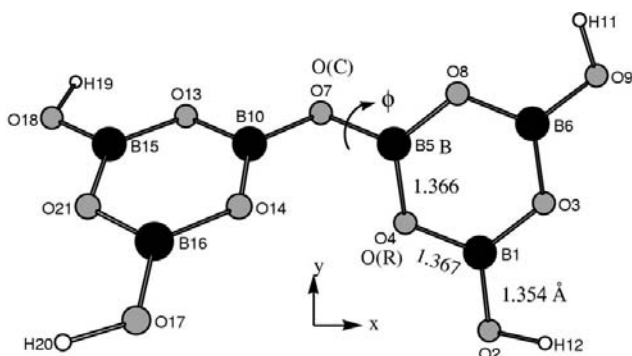**Figure 13**
A model of $B_2O_3$ glass for simulating the work of Jellison *et al.* (1977). This $B_6O_6(OH)_4$ structure was determined with *ab initio* HF/STO-3G. B5—O8 1.367, B5—O7 1.349, O7—B10 1.349 Å, B5—O7—B10 130.50°. Twist angle $\varphi = 27.78°$. O(R), O(C) and B are notations used by Jellison *et al.* (1977). Bond distances are given in Å.

**Table 15**
Calculated valences ($V$) and net charges ($c$) of O(R), B and O(C) in $B_6O_6(OH)_4$ drawn in Fig. 13.

| Method | O(R) | | B | | O(C) | |
|---|---|---|---|---|---|---|
| | $V$ | $c$ | $V$ | $c$ | $V$ | $c$ |
| DVX$_\alpha$ | 2.009 | −0.720 | 2.928 | 1.064 | 2.050 | −0.703 |
| HF/STO-3G | 2.299 | −0.420 | 3.317 | 0.625 | 2.316 | −0.425 |
| HF/3-21G | 1.898 | −0.779 | 2.885 | 1.166 | 1.900 | −0.793 |
| HF/6-31G | 1.773 | −0.771 | 2.923 | 1.151 | 1.759 | −0.787 |

orbital of O(C). Note that non-negligible amounts of $2p_z$ orbital contributions from other atoms are mixed into the $\pi$-orbital of O(C) (for example, 0.2007 of B10 Z). That is, the $\pi$-lone pair orbitals of O(C) are partly de-localized and it is this that causes the population to be less than 2. [This partial de-localization also occurs on O(R), but this effect was taken into account in the estimation of the population on the $\pi$-orbital of O(R)]. Hence, the valence of O(C) in Table 2, 1.492, is an underestimated value. The actual value should be close to that of O(R), since there is no large difference between the calculated $\pi$-orbital populations of O(C) and O(R) (1.745 and 1.691, respectively). Thus, the valence of O(C) should be close to 2 and consequently the net charge of O(7) should be *ca* −0.7.

The corrected valence of O(C) can be estimated in another way. There may be few problems in the analysis for the B atom, compared with the analysis for O(C), since the sign-ambiguity of the asymmetric factor for the electric field gradient makes little difference to the orbital populations on the B atom. An important point is that the B atom $\pi$-orbital ($2p_z$) has a significant population of 0.360 (see §5.2). The corresponding calculated values are 0.437 from DVX$_\alpha$, which is not too different from 0.360. Hence, it is believed that the results for the B atom are essentially reliable and thus the value of its valence (2.945 or 2.949) is correct. Since O(C) bonds to the two B atoms, its valence should be nearly 2 × 2.945/3 = 1.96 ≃ 2. This conclusion is also applicable to O(R), since O(R) also bonds to two B atoms. Thus, following the discussion in the previous paragraph, we can conclude that the work of Jellison *et al.* (1977) suggests that the B and O atoms in $B_2O_3$ glass have valences close to their classical values.

Jellison *et al.* (1977) provide a criterion which can be used to determine which molecular-orbital method gives the valences which best correspond to the experimental ones. Table 15 compares the valences and the net charges calculated from the four molecular-orbital methods and it is clear that DVX$_\alpha$ gives the best match to the experimental values. Hence, at the present stage, we conclude that DVX$_\alpha$ gives the best estimates of the actual atomic valences in molecules and solids.

**5.6.2. Absolute bond valence for oxides.** It should be noted that all the numerical results for the valences ($V_A^b$, $V_A$) in the M—O systems treated in this paper are close to the absolute values of the oxidation numbers of the atoms involved. For example, the valences of Be, B, Al and Si in Table 2 are 1.96, 2.96, 3.26 and 4.36. The valence of Fe in $[Fe(H_2O)_6]^{2+}$ is 1.96 (Table 9), in contrast with the values in the $Fe^{2+}$-pyridine and

$Fe^{2+}$-cyano complexes. In beryl, the calculated oxygen valences $V_O^b$ are 1.93 and 1.96, and the corresponding total valences are 2.05 and 2.07, respectively. The calculated oxygen valences $V_O^b$ for O(R) and O(C) in $B_6O_6(OH)_4$ are 1.88 and 1.91, respectively, and the corresponding total valences $V_O$ are 2.01 and 2.05. On the other hand, the values for $V_{Al}^b$ and $Cl_b$ in $Al_2Cl_6$ are 3.72 and 1.35, respectively. Moreover, it has been found that in $Al_2Br_6$, the valence of Al is 4.06, which is far from the formal oxidation number for $Al^{3+}$. $V_{Si}^b$ values in $SiF_4$, $SiCl_4$ and $SiBr_4$ are 4.40, 4.63 and 4.95, respectively: here the stronger covalent character is probably responsible for the larger deviations of the calculated valences from the formal oxidation numbers. The conclusion (see §5.6.1) is that the valences from the $DVX_\alpha$ method are close to the experimental values. *Hence, it can be predicted that the valences of atoms in oxides are approximately equal to the absolute values of the oxidation numbers of the atoms.* This prediction states that the definition (34) is numerically applicable to oxides. Moreover, this explains why the ionic interpretation for the bond-valence rule apparently works well for oxides and why the bond-valence sum rule obeys the electroneutral principle (Pauling, 1960). Of course, in order to examine this prediction, further investigations on the orbital population analysis for atoms in solids are desirable.

## 6. Concluding remarks

We have seen that the Okada bond order $D_{MX}$ satisfies the three requirements (i), (ii) and (iii) mentioned in §1, and that (33) brings nearly the same results as the bond valences from the empirical relations. Hence, we conclude that the quantity $x$ referred to in §1 is the Okada bond order and the relative definition (33) is a quantum-mechanical representation of the bond valence. Consideration of the mechanism of the bond-valence sum rule leads to an understanding of the bond-valence sum rule as a covalent bond effect caused by the tendency of atoms in molecules or crystals to adopt as spherical an electron population state as possible. The magnitude of the $d$-orbital contribution is an important factor affecting whether the conventional form of the bond-valence sum rule can be used. Moreover, it has been shown that the atomic valences in oxides are possibly close to the absolute values of the oxidation numbers. If we therefore choose the absolute definition as given in (34), the bond valence can be identified as the Okada bond order. This definition may be more chemically significant than the relative definition.

## APPENDIX A
### A1. Merits of the $DVX_\alpha$ method

Application of the $DVX_\alpha$ method to the valence analysis is not yet commonplace, but there are at least three factors which favour the use of $DVX_\alpha$. The first factor is that $DVX_\alpha$ is easily applicable to all types of compound (not only organic compounds, but also inorganic compounds including transition metal complexes and metal-alloys), as stated in §4. The second is that this method gives reasonable Okada bond orders and net charges. Table 16 shows the comparison of the *DVSCAT* results with *ab initio* HF results. In this table we can find some unreasonable values (in bold). In the $N_2$ molecule the valences of N from 3-21G and 6-31G are unreasonably small, since $N_2$ is a homonuclear diatomic molecule with a true triple bond. For the C atoms in butadiyne (HCCCCH), valence values greater than four occur for the C atoms (this may be a proper feature of the split-valence-type basis functions). In $CCl_4$, the 3-21G and 6-31G calculations result in positive charges on the Cl atoms, also unlikely. On the contrary, the valences from STO-3G (or STO-3G*) are reasonable on the whole, as was pointed out by Lendvay (1989). However, the minimal basis functions give another type of improbable valence. For LiF(g) STO-3G predicts unreasonably large valences of 1.346 for both Li and F. As this typical example shows, this basis function tends to overestimate the covalent interaction in systems where considerable ionic character is present, consequently yielding unrealistically large valences and small net charges. [This phenomenon may be largely due to the so-called 'basis-set superposition error' (BSSE; Davidson & Feller, 1986)]. In contrast, for every type of system *DVSCAT* produces realistic values for both valences and net charges, as shown in Table 16. The final factor is that *ab initio* HF incorporates Lewis-pair-related quantities including the significant inner electron contribution. For example, the *ab initio* HF/STO-3G* calculation for $[Al(OH)_6]^{3-}$ gives the orbital populations on 1$s$, 2$s$, 2$p_x$, 2$p_y$ and 2$p_z$ of the Al as 2.000, 1.987, 1.962, 1.962 and 1.962, respectively, all significantly less than 2.000, except for the 1$s$ population. This result indicates that the 2$s$ and the 2$p$ orbitals are contributing significantly to the Al—O bonds. Once the inner electrons are taken into account, the behaviors of the valence electron parts of the Lewis-pair-related quantities, chemically important parts, are almost hidden. Moreover, eliminating the inner electron contributions from output $- B_{AB}$ is impossible since the contents of the $B_{AB}$ are not output. Meanwhile, *DVSCAT* gives orbital populations of 2.000 for all the inner shells of the Al. Thus, *DVSCAT* gives results where the valence electron contributions are completely separated from those of the inner electrons.

**Table 16**
$DVX_\alpha$ gives chemically realistic valences ($V_A^b$) and net charges ($c_A$).

Values in bold are regarded as unrealistic. STO-3G*, 3-21G* and 6-31G* were applied to Si, Na and Cl.

| | | $V_A^b$ | | | | $c_A$ | | | |
|---|---|---|---|---|---|---|---|---|---|
| | $A$ | $DVX_\alpha$ | STO-3G | 3-21G | 6-31G | $DVX_\alpha$ | STO-3G | 3-21G | 6-31G |
| $F_2$ | F | 1.000 | 1.000 | 1.003 | 1.003 | 0.000 | 0.000 | 0.000 | 0.000 |
| $N_2$ | N | 2.999 | 3.000 | **2.791** | **2.635** | 0.000 | 0.000 | 0.000 | 0.000 |
| $CH_4$ | C | 3.967 | 3.964 | 3.736 | 3.840 | −0.287 | −0.251 | −0.787 | −0.621 |
| HCCCCH | $C_c$ | 3.988 | 3.993 | **4.180** | **4.508** | 0.009 | −0.035 | −0.260 | −0.132 |
| | $C_H$ | 3.725 | 3.822 | 3.833 | **4.261** | −0.141 | −0.082 | −0.131 | −0.291 |
| $CO_2$ | C | 3.841 | 3.934 | 3.606 | 3.648 | 0.788 | 0.465 | 1.083 | 0.862 |
| | O | 1.921 | 1.967 | 1.803 | 1.824 | −0.394 | −0.233 | −0.541 | −0.431 |
| $CCl_4$ | C | 3.845 | 3.860 | 3.638 | 3.867 | 0.551 | 0.138 | **−0.468** | **−0.364** |
| | Cl | 0.961 | 0.965 | 0.909 | 0.967 | −0.138 | −0.035 | **0.117** | **0.091** |
| $CF_4$ | C | 3.626 | 3.856 | 3.588 | 3.640 | 1.188 | 0.622 | 1.516 | 1.384 |
| | F | 0.907 | 0.964 | 0.897 | 0.910 | −0.297 | −0.156 | −0.379 | −0.346 |
| $H_2O$ | O | 1.740 | 1.908 | 1.811 | 1.607 | −0.704 | −0.331 | 3.588 | −0.792 |
| $Si(OH)_4$ | Si | 4.288 | 4.692 | 4.064 | 4.088 | 1.248 | 0.694 | 1.395 | 1.373 |
| | O | 1.901 | 2.082 | 1.792 | 1.754 | −0.693 | −0.391 | −0.766 | −0.820 |
| $BF_3$ | B | 2.893 | 3.300 | 2.936 | 2.827 | 1.099 | 0.649 | 1.169 | 1.201 |
| LiF(g) | Li | 0.654 | **1.346** | 0.763 | 0.491 | 0.646 | 0.228 | 0.565 | 0.743 |
| NaCl(g) | Na | 0.842 | **1.108** | 0.578 | 0.623 | 0.524 | 0.318 | 0.703 | 0.662 |

## References

Aarset, K., Shen, Q., Thomassen, H., Richardson, A. D. & Hedberg, K. (1999).*J. Phys. Chem. A*, **103**, 1644–1652.

Adachi, H., Tsukada, M. & Satoko, C. (1978). *J. Phys. Soc. Jpn*, **45**, 875–882.

Armstrong, D. R., Perkins, P. G. & Stewart. J. J. (1973). *J. Chem. Soc. Dalton Trans.* pp. 838–840.

Brown, I. D. (2002). *The Chemical Bond in Inorganic Chemistry: The Bond Valence Model.* IUCr Monograph on Crystallography 12. Oxford University Press.

Brown, I. D. & Altermatt, D. (1985). *Acta Cryst.* B**41**, 244–247.

Brown, I. D. & Shannon, R. D. (1973). *Acta Cryst.* A**29**, 266–282.

Burdett, J. K. & Hawthorn, F. C. (1993). *Am. Mineral.* **78**, 884–892.

Burdett, J. K. & McLarnan, T. J. (1984). *Am. Mineral.* **69**, 601–621.

Buss, B. & Krebs, B. (1971). *Inorg. Chem.* **10**, 2795–2800.

Cooper, W. F., Larsen, F. K. & Coppens, P. (1973). *Am. Miner.* **58**, 21–31.

Coulson, C. A. (1961). *VALENCE*, 2nd ed. Oxford: Clarendon Press.

Davidson, E. R. & Feller, D. (1986). *Chem. Rev.* **86**, 681–696.

Dent Glasser, L. S. & Giovanoli, R. (1972a). *Acta Cryst.* B**28**, 519–524.

Dent Glasser, L. S. & Giovanoli, R. (1972b). *Acta Cryst.* B**28**, 760–763.

Donnay, G. & Donnay, J. D. H. (1973). *Acta Cryst.* B**29**, 1417–1425.

Edge, R. A. & Taylor, H. F. (1971). *Acta Cryst.* B**27**, 594–601.

Edmiston, C. & Ruedenberg, K. (1963). *Rev. Mod. Phys.* **35**, 457–465.

Giambiagi, M., Giambiagi, M., Grempel. D. R. & Heymann, C. D. (1975). *J. Chim. Phys.* **72**, 15–22.

Gibbs, G. V. (1982). *Am. Mineral.* **67**, 421–450.

Gillespie, R. J. & Nyholm, R. S. (1957). *Q. Rev. Chem. Soc.* **11**, 339–380.

Gopinathan, M. S. & Jug. K. (1983a). *Theoret. Chim. Acta (Berlin)*, **63**, 497–509.

Gopinathan, M. S. & Jug, K. (1983b). *Theoret. Chim. Acta (Berlin)*, **63**, 511–527.

Granovsky, A. A. (1999). http://classic.Chem.msu.su/gran/gamess/index.html.

Hazell, A. C. (1966). *Acta Chem. Scand.* **20**, 165–169.

Jansen, L., Chandran, L. & Block, R. (1992). *J. Mol. Struct. (Theochem.)* **260**, 81–98.

Jellison, G. E. Jr, Panek, L. W., Bray, P. J. & Rouse, G. B. Jr (1977). *J. Chem. Phys.* **66**, 802–812.

Julg, A. (1978). *Crystals as Giant Molecules: Lecture Notes in Chemistry*, edited by G. Berthier, M. J. S. Dewar, H. Fischer, K. Fukui, H. Hartmann, H. H. Jaffé, J. Jortner, W. Kutzelnigg, K. Ruedenberg, E. Scrocco & W. Zeil, Vol. 9. Berlin, Heidelberg, New York: Springer-Verlag.

Kowada, Y., Tanaka, I., Nakamatsu, H. & Mizuno, M. (1998). *Hazimeteno Denshijoytai Keisan* (*Electronic Structure Calculations for Beginners*). Tokyo: Sankyo-Syuppan; http://www.Sci.hyogo-u.ac.jp/ykowada/.

Kutschabsky, L. (1969). *Acta Cryst.* B**25**, 1811–1816.

Lendvay, G. (1989). *J. Phys. Chem.* **93**, 4422–4429.

Löwdin, P. O. (1955a). *Phys. Rev.* **97**, 1474–1489.

Löwdin, P. O. (1955b). *Phys. Rev.* **97**, 1490–1508.

Mayer, I. (1983). *Int. J. Quantum Chem.* **23**, 341–363.

Mayer, I. (1986a). *Int. J. Quantum Chem.* **29**, 73–84.

Mayer, I. (1986b). *Int. J. Quantum Chem.* **29**, 477–483.

Mayer, I. (1987). *J. Mol. Struct (Theochem.)* **149**, 81–89.

Mohri, F. (2000). *Acta Cryst.* B**56**, 626–638.

Morimoto, N. (1956). *Mineral. J.* **2**, 1–18.

Morosin, B. (1972). *Acta Cryst.* B**28**, 1899–1903.

Mulliken, R. S. (1955). *J. Chem. Phys.* **23**, 1841–1846.

Nakagawa, K. (2000). *Adv. Quant. Chem.* **37**, 365–374.

Newton, M. D. (1977). *Applications of Electronic Structure Theory*, ch. 6, edited by H. F. Schaefer III. New York: Plenum Press.

Okada, T. (1977). *Kagaku no Ryoiki* (*Chemistry Field*), **31**, 1007–1015.

Okada, T. & Fueno, T. (1975). *Bull. Chem. Soc. Jpn*, **48**, 2025–2032.

Okada, T. & Fueno, T. (1976). *Bull. Chem. Soc. Jpn*, **49**, 1524–1530.

Pauling, L. (1929). *J. Am. Chem. Soc.* **51**, 1010–1026.

Pauling, L. (1960). *The Nature of the Chemical Bond*, 3rd ed. Cornell University Press.

Pople, J. A. & Segal, G. A. (1966). *J. Chem. Phys.* **44**, 3290–3296.

Preiser, C., Lösel, J., Brown, I. D., Kunz, M. & Skowron, A. (1999). *Acta Cryst.* B**55**, 698–711.

Rutherford, J. S. (1998). *Acta Cryst.* B**54**, 204–210.

Schmidt, M. W., Baldridge, K. K., Boatz, J. A., Elbert, S. T., Gordon, M. S., Jensen, J. H., Koseki, S., Matsunaga, N., Nguyen, K. A., Su, S., Windus, T. L., Dupuis, M. & Montgomery, J. A. (1993). *J. Comput. Chem.* **14**, 1347–1363; http://www.msg.ameslab.gov/GAMESS/GAMESS.html.

See, R. F., Kruse, R. A. & Strub, W. M. (1998). *Inorg. Chem.* **37**, 5369–5375.

Siddarth, P. & Gopinathan, M. S. (1990). *Int. J. Quantum. Chem.* **37**, 685–699.

The Chemical Society of Japan (1984). *Kagaku-binran* (*Chemistry Data*), 3rd ed. Tokyo: Maruzen.

Suzuya, K., Yoneda, Y., Kohara, S. & Umesaki, N. (2000). *Phys. Chem. Glasses*, **41**, 282–285.

Tossel, J. A. (1987). *Phys. Chem. Miner.* **14**, 320–326.

Urusov, V. M. (1995). *Acta Cryst.* B**51**, 641–649.

Wiberg, K. B. (1968). *Tetrahedron*, **24**, 1083–1096.

Youngman, R. E., Haubrich, S. T., Zwanzinger, J. W., Janicke, M. T. & Chmelka, B. F. (1995). *Science*, **269**, 1416–1420.

Zachariasen, W. H. (1954). *Acta Cryst.* **7**, 305–310.